Received: 26 March 2021 | Revised: 14 May 2021 | Accepted: 2 June 2021

DOI: 10.1002/ar.24704

SPECIAL ISSUE ARTICLE

The Anatomical Record

WILEY

Cranial and endocranial anatomy of a three-dimensionally preserved teleosauroid thalattosuchian skull

Eric W. Wilberg[1] | **Alexander R. Beyl**[1] | **Stephanie E. Pierce**[2] | **Alan H. Turner**[1]

[1]Department of Anatomical Sciences, Stony Brook University, Stony Brook, New York, USA

[2]Museum of Comparative Zoology and Department of Organismic and Evolutionary Biology, Harvard University, Cambridge, Massachusetts, USA

Correspondence
Eric W. Wilberg, Department of Anatomical Sciences, Health Sciences Center, T8 (083), Stony Brook University, Stony Brook, New York, 11794, USA.
Email: eric.wilberg@stonybrook.edu

Funding information
National Science Foundation, Grant/Award Number: DEB 1754596

Abstract

Thalattosuchians represent one of the several independent transitions into the marine realm among crocodylomorphs. The extent of their aquatic adaptations ranges from the semiaquatic teleosauroids, superficially resembling extant gharials, to the almost cetacean-like pelagic metriorhynchids. Understanding the suite of osteological, physiological, and sensory changes that accompanied this major transition has received increased attention, but is somewhat hindered by a dearth of complete three-dimensionally preserved crania. Here, we describe the cranial and endocranial anatomy of a well-preserved three-dimensional specimen of *Macrospondylus bollensis* from the Toarcian of Yorkshire, UK. The trigeminal fossa contains two similar-sized openings separated by a thin lamina of prootic, a configuration that appears unique to a subset of teleosauroids. *Macrospondylus bollensis* resembles other thalattosuchians in having pyramidal semicircular canals with elongate cochlear ducts, enlarged carotid canals leading to an enlarged pituitary fossa, enlarged orbital arteries, enlarged endocranial venous sinuses, reduced pharyngotympanic sinuses, and a relatively straight brain with a hemispherical cerebral expansion. We describe for the first time the olfactory region and paranasal sinuses of a teleosauroid. A relatively large olfactory region suggests greater capacity for airborne olfaction in teleosauroids than in the more aquatically adapted metriorhynchoids. Additionally, slight swellings in the olfactory region suggest the presence of small salt glands of lower secretory capacity than those of metriorhynchoids. The presence of osteological correlates for salt glands in a teleosauroid corroborates previous hypotheses that these glands originated in the common ancestor of Thalattosuchia, facilitating their rapid radiation into the marine realm.

KEYWORDS

Crocodylomorpha, endocranial anatomy, marine adaptation, neuroanatomy, Thalattosuchia

1 | INTRODUCTION

Thalattosuchians are an extinct clade of crocodylomorph archosaurs that were a major component of coastal marine, estuarine, and pelagic faunas from the Lower Jurassic through Lower Cretaceous (Buffetaut, 1980, 1982; Hua & Buffetaut, 1997; Johnson, Young, & Brusatte, 2020a, 2020b; Wilberg, 2015a; Young, Brusatte, & Ruta, 2010). While the

origin of the clade and its position within Crocodylomorpha remains somewhat contentious (Brochu, 2001; Clark, 1986, 1994; Jouve, 2009; Leardi, Pol, & Clark, 2017; Pol & Gasparini, 2009; Wilberg, 2015b), the monophyly of Thalattosuchia is not. Thalattosuchia comprises two clades: Teleosauroidea and Metriorhynchoidea (Hua & Buffetaut, 1997; Vignaud, 1995; Young et al., 2012). Of these, metriorhynchoids became highly adapted to the pelagic realm, showing major cranial, appendicular, and axial skeletal changes (Schwab et al., 2020; Wilberg, 2015a; Young et al., 2010). The teleosauroids, however, retained a skull architecture and body plan more similar to semi-aquatic crocodyliforms, though a range of habitats and ecomorphologies are present within the group (Johnson et al., 2020a; Wilberg, Turner, & Brochu, 2019).

Teleosauroidea was among the earliest fossil groups studied (e.g., Chapman, 1758; Wooler, 1758) and received much attention during the 19th and early 20th centuries (e.g., Cuvier, 1824; Geoffroy Saint-Hilaire, 1825; Eudes-Deslongchamps, Eudes-Deslongchamps, 1863-1869; Andrews, 1909, 1913). However, it received less study during the latter part of the 20th century (but see Westphal, 1961, 1962; Buffetaut, 1980, 1982; Vignaud, 1995, Hua & de Buffrenil, 1996; Hua & Buffetaut, 1997). A renaissance of thalattosuchian research began in the early 21st century (e.g., Aiglstorfer, Havlik, & Herrera, 2020; Barrientos-Lara, Alvarado-Ortega, & Fernández, 2018; Barrientos-Lara, Herrera, Fernández, & Alvarado-Ortega, 2016; Buchy, Vignaud, Frey, Stinnesbeck, & Gonzalez Gonzalez, 2006; Buchy, Young, & Andrade, 2013; Cau & Fanti, 2011; Fernández & Gasparini, 2000, 2008; Fernández & Herrera, 2009; Foffa & Young, 2014; Gasparini, Cichowolski, & Lazo, 2005; Gasparini, Pol, & Spalletti, 2006; Gasparini, Vignaud, & Chong, 2000; Herrera et al., 2009, 2013a,b,c, 2015, 2017; Hua, 2020; Hua, Vignaud, Atrops, & Clément, 2000; Leardi, Pol, & Fernández, 2012; Mueller-Töwe, 2006; Ösi, Young, Galácz, & Rabi, 2018; Parrilla-Bel, Young, Moreno-Azanza, & Canudo, 2013; Pierce, Angielczyk, & Rayfield, 2009a, 2009b; Pierce & Benton, 2006; Pierce, Williams, & Benson, 2017; Pol & Gasparini, 2009; Wilberg, 2015a, 2015b; Young et al., 2010, 2012; Young & Andrade, 2009; Young, Andrade, Cornée, Steel, & Foffa, 2014; Young, Andrade, Etches, & Beatty, 2013; Young, Bell, Andrade, & Brusatte, 2011), with a recent focus on the anatomy, taxonomy, and phylogenetic relationships of teleosauroids (Brusatte et al., 2016; Foffa, Johnson, Young, Steel, & Brusatte, 2019; Herrera, Leardi, & Fernandez, 2018; Johnson et al., 2017, 2020a, 2020b; Johnson, Young, Steel, & Lepage, 2015; Jouve, 2009; Martin et al., 2019; Martin & Vincent, 2013; Sachs, Johnson, Young, & Abel, 2019; Young et al., 2014; Young, Beatty, Brusatte, & Steel, 2015). This research has helped elucidate the previously unrecognized morphological and ecological diversity present among teleosauroids. Unfortunately, nearly all teleosauroid skulls exhibit strong dorsoventral compression as a result of the fossilization process. This preservational bias hinders our understanding of the cranial and neuroanatomical evolution for the clade.

Thalattosuchians represent one of five independent transitions to the marine realm within Crocodylomorpha, and include the only crocodylomorph group to exploit pelagic ecosystems (Wilberg et al., 2019). As such, they are an ideal group to investigate the osteological and neuroanatomical changes associated with this transition. Schwab et al. (2020) showed that the inner ear of thatattosuchians changed dramatically as they transitioned from terrestrial ancestors to more coastal marine (teleosauroids and early diverging metriorhynchoids) and pelagic (metriorhynchids) ecomorphs. Recent studies based on computed tomography (CT) have increased our knowledge of the neuroanatomy, pneumatic diverticula, and cranial vasculature of teleosauroids (Brusatte et al., 2016; Herrera et al., 2018) but these pertained to partial braincases or incomplete skulls. Among the best known teleosauroids is *Macrospondylus* ("*Steneosaurus*") *bollensis* Jäger, 1828. It is represented by hundreds of specimens primarily recovered from the Posidonia Shale and Whitby Mudstone (Westphal, 1961, 1962). While some of these specimens are exquisitely preserved often as articulated nearly complete skeletons, almost all are preservationally compressed and many are preserved as slab specimens. This preservational bias prevents complete descriptions of some aspects of three-dimensional morphology.

In this contribution we describe the cranial and endocranial anatomy of a three-dimensionally preserved specimen of *Macrospondylus bollensis* (MCZ VPRA-1063), including a nearly complete skull and mandible, missing only the anterior part of the rostrum. The relatively complete nature of MCZ VPRA-1063 provides an opportunity to consider details of skull, braincase, and mandible morphology that are poorly preserved or not preserved in many other specimens in terms of osteology, endocast shape, bony labyrinth morphology, cranial vasculature, and pneumatization. We present the details of the olfactory region and paranasal sinuses for the first time in a teleosauroid, allowing comparisons with metriorhynchoids, which housed enlarged exocrine salt glands in this region (Fernández & Herrera, 2009; Herrera, Fernández, & Gasparini, 2013b; Pierce et al., 2017).

A note on teleosauroid taxonomy: The taxonomy of Teleosauroidea has recently undergone a comprehensive and major revision (Johnson et al., 2020a, 2020b). In this contribution, we follow the taxonomy of Johnson

et al. (2020a, 2020b) but for clarity, make note of older names upon first mention of the taxon where applicable.

Institutional abbreviations: AMNH FARB, American Museum of Natural History, Fossil Amphibians, Reptiles, and Birds, New York, New York, USA; BRLSI, Bath Royal Literary and Scientific Institution, Bath, UK; CAMSM, Sedgwick Museum of Earth Science, Cambridge, UK; GPIT, Paläontologische Sammlung der Eberhard Karls Universität, Tübingen, Germany; IVPP, Institute of Vertebrate Paleontology and Paleoanthropology, Beijing, China; MCZ, Museum of Comparative Zoology, Harvard University, Cambridge, Massachusetts, USA; MNHN, Muséum National d'Histoire Naturelle, Paris, France; NHMUK, Natural History Museum, London, UK; NJSM, New Jersey State Museum, Trenton, New Jersey, USA; OUMNH, Oxford University Museum of Natural History, Oxford, UK; PRC, Palaeontological Research and Education Centre, Maha Sarakham University, Maha Sarakham, Thailand; SMNS, Staatliches Museum für Naturkunde, Stuttgart, Baden-Württemberg, Germany; SNSB-BSPG, Staatliche Naturwissenschaftliche Sammlungen Bayerns-Bayerische Staatssammlung für Paläontologie und Geologie, Munich, Germany; UH Urweltmuseum Hauff Holzmaden, Germany; UOMNH, University of Oregon Museum of Natural and Cultural History, Eugene, OR, USA.

2 | MATERIALS AND METHODS

2.1 | Specimen

This study focuses on the partial cranium and mandible of MCZ VPRA-1063 from the Toarcian (Early Jurassic) of Yorkshire (near Whitby), United Kingdom (UK). It was acquired by an exchange with Tufts College, though no further information about the specimen is available. We assign this specimen to *Macrospondylus bollensis* on the basis of the following combination of characteristics: ornamentation in a radial pattern of pits on the frontal, extending slightly onto the prefrontals; shallow groove or trough present between the nasals where they articulate with the anterior process of the frontal; presence of a small ovoid antorbital fenestra, bordered by the lacrimal, jugal, and maxilla; jugal excluded, or nearly so, from the orbital margin by contact between a posterior process of the lacrimal and anteroventral process of the postorbital; trapezoidal supratemporal fenestrae approximately 1.25 times longer than wide. In terms of three-dimensional preservation, general bone color and texture, and matrix characteristics, it closely resembles NHMUK PV OR 14436 and an unnumbered CAMSM specimen, both attributed to *Macrospondylus bollensis* and originating from the Toarcian of Whitby, Yorkshire, UK. MCZ VPRA-1063 is, however, slightly better preserved and more completely prepared.

2.2 | Computed tomography visualization

MCZ VPRA-1063 was CT scanned on a LightSpeed VCT Scanner (GE Healthcare, Waukesha, WI) located in the Stony Brook University Hospital using a voltage of 140 kv and a current 500 mA acquiring 640 images with a slice thickness of 0.625 and a 0.500 mm interslice thickness. Dicom files were imported into Avizo 2020.1 (Thermo Scientific). Three dimensional digital models of the endocranial cavity, endosseous labyrinth, antorbital region, and pharyngotympanic space were created using manual image segmentation, following the best practices of Balanoff et al. (2016). Due to the varying degrees of density differences between the bone and remaining matrix, as well as the presence of beam hardening in places, frequent adjustments to grayscale thresholds were necessary. The brush tool was used to select the endocranial space at bone boundaries and the space within the boundary was captured using the fill command. CT data and digital models available upon request at https://mczbase.mcz.harvard.edu/guid/MCZ:VP:VPRA-1063 (Requests should be directed to mcz_vertebratepaleo@fas.harvard.edu).

3 | RESULTS

General form and preservation: The skull and mandible are three-dimensionally preserved and in articulation (Figures 1–8). Both the skull and mandible are fractured approximately halfway along the rostrum (based on comparisons against specimens with complete rostra; e.g., GPIT Re 1193/1) and the anterior half of each is missing (though a small part of the anterior tip of the right dentary is present). Finite element modelling has shown this to be a point of weakness in teleosauroid snouts and specimens with breakage in this region are common (Pierce et al., 2009b). The preserved bone is dark colored with sutures generally well visible in most areas. Both the right retroarticular process and large portions of both jugals along the lower temporal bars are missing. The area surrounding the braincase and orbits has been completely prepared, but matrix has been left between the palatal surface and mandible, precluding description of this area.

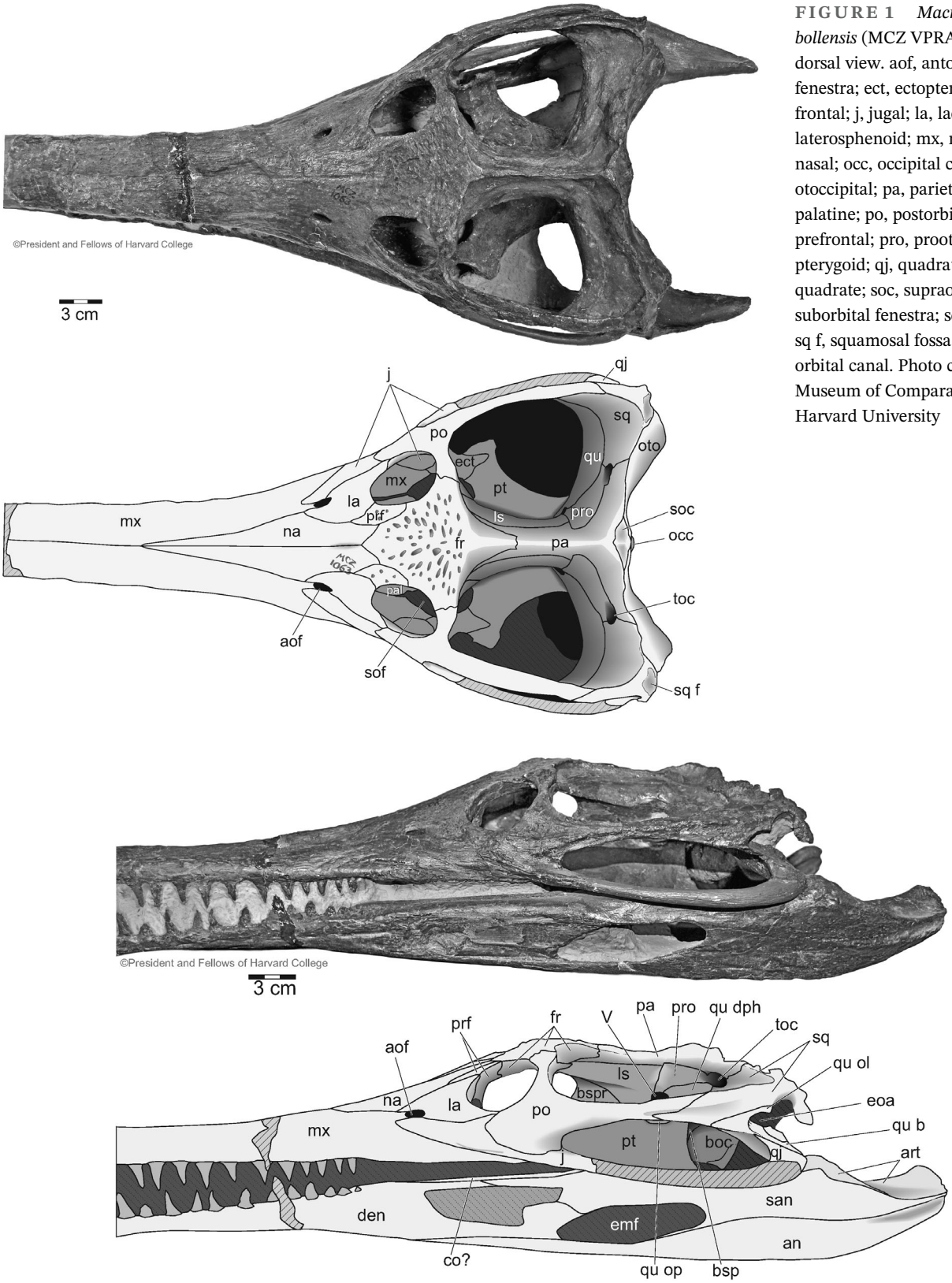

FIGURE 1 *Macrospondylus bollensis* (MCZ VPRA-1063) in dorsal view. aof, antorbital fenestra; ect, ectopterygoid; fr, frontal; j, jugal; la, lacrimal; ls, laterosphenoid; mx, maxilla; na, nasal; occ, occipital condyle; oto, otoccipital; pa, parietal; pal, palatine; po, postorbital; prf, prefrontal; pro, prootic; pt, pterygoid; qj, quadratojugal; qu, quadrate; soc, supraoccipital; sof, suborbital fenestra; sq, squamosal; sq f, squamosal fossa; toc, temporo-orbital canal. Photo credit: Museum of Comparative Zoology, Harvard University

FIGURE 2 *Macrospondylus bollensis* (MCZ VPRA-1063) in left lateral view. an, angular; aof, antorbital fenestra; art, articular; boc, basioccipital; bsp, basisphenoid; bspr, basisphenoid rostrum; co?, coronoid?; den, dentary; emf, external mandibular fenestra; eoa, external otic aperture; fr, frontal; j, jugal; la, lacrimal; ls, laterosphenoid; mx, maxilla; na, nasal; pa, parietal; po, postorbital; prf, prefrontal; pro, prootic; pt, pterygoid; qj, quadratojugal; qu b, quadrate body; qu dph, dorsal primary head of quadrate; qu ol, otic lamina of quadrate; qu op, orbital process of quadrate; san, surangular; sq, squamosal; toc, temporo-orbital canal; V, trigeminal foramen. Photo credit: Museum of Comparative Zoology, Harvard University

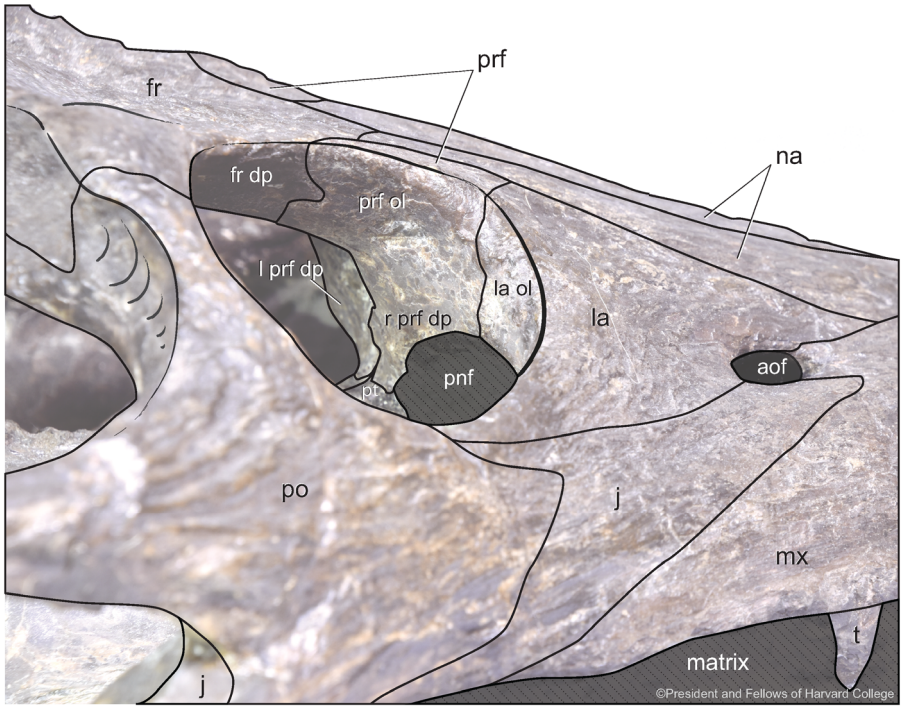

FIGURE 3 Photograph with superimposed line interpretation of the right orbital and antorbital region of *Macrospondylus bollensis* (MCZ VPRA-1063) in oblique lateral view. aof, antorbital fenestra; fr, frontal; fr dp, descending process of frontal; j, jugal; l prf dp, descending process of left prefrontal; la, lacrimal; la ol, orbital lamina of lacrimal; mx, maxilla; na, nasal; pnf, postnasal fenestra; po, postorbital; prf, prefrontal; prf ol, orbital lamina of prefrontal; r prf dp, descending process of right prefrontal; pt, pterygoid; t, tooth. Photo credit: Museum of Comparative Zoology, Harvard University

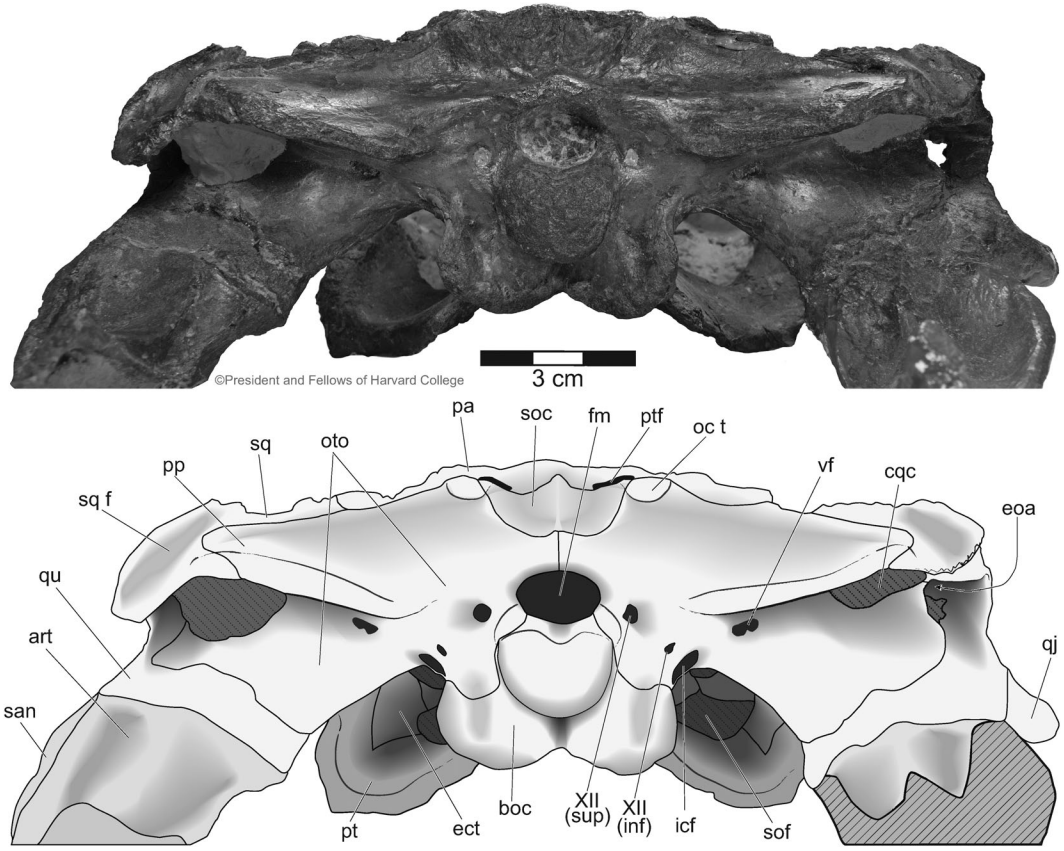

FIGURE 4 *Macrospondylus bollensis* (MCZ VPRA-1063) in occipital view. Solid diagonal lines indicate reconstructed region; dotted diagonal lines represent remaining matrix. art, articular; cqc, cranioquadrate canal; ect, ectopterygoid; eoa, external otic aperture; fm, foramen magnum; icf, internal carotid foramen; oc t, occipital tuberosity; oto, otoccipital; pa, parietal; pp, paroccipital process; pt, pterygoid; ptf, posttemporal fenestra; qj, quadratojugal; qu, quadrate; san, surangular; soc, supraoccipital; sof, suborbital fenestra; sq, squamosal; sq f, squamosal fossa; vf, vagus foramen; XII (sup), superior hypoglossal foramen; XII (inf), inferior hypoglossal foramen. Photo credit: Museum of Comparative Zoology, Harvard University

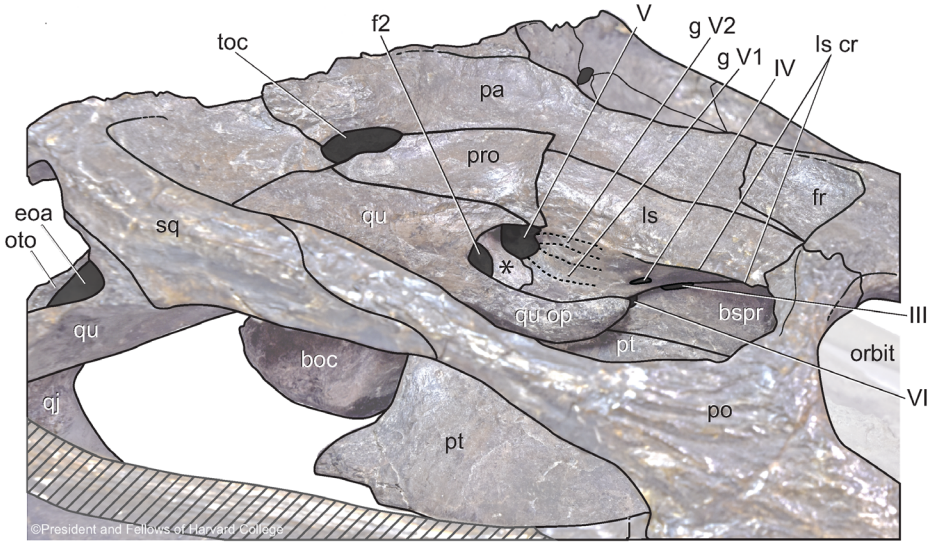

FIGURE 5 *Macrospondylus bollensis* (MCZ VPRA-1063) in oblique dorsolateral view showing details of the lateral wall of the braincase. * indicates the strut of the prootic separating the trigeminal foramen from the paratympanic sinus. boc, basioccipital; bspr, basisphenoid rostrum; eoa, external otic aperture; f2, "Foramen 2"; fr, frontal; g V1, groove for ophthalmic nerve; g V2, groove for maxillary nerve; III, oculomotor foramen; IV, trochlear foramen; j, jugal; ls, laterosphenoid; ls cr, laterosphenoid crest; oto, otoccipital; pa, parietal; po, postorbital; pro, prootic; pt, pterygoid; qj, quadratojugal; qu, quadrate; qu op, orbital process of quadrate; sq, squamosal; toc, temporo-orbital canal; V, trigeminal foramen; VI, abducens foramen. Photo credit: Museum of Comparative Zoology, Harvard University

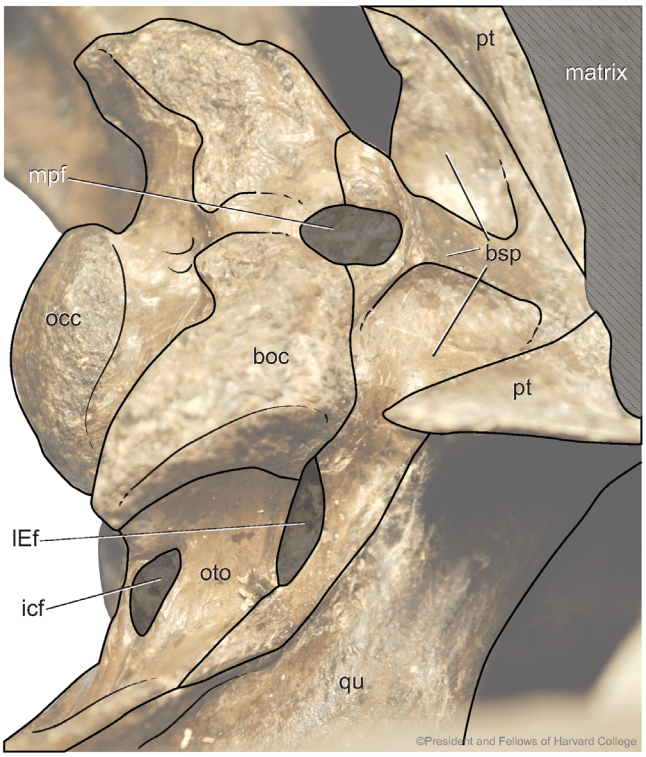

FIGURE 6 Photograph with superimposed line interpretation showing details of the posterior portion of the ventral surface of *Macrospondylus bollensis* (MCZ VPRA-1063) in oblique view. boc, basioccipital; bsp, basisphenoid; icf, internal carotid foramen; lEf, lateral Eustachian foramen; mpf, median pharyngeal foramen; occ, occipital condyle; oto, otoccipital; pt, pterygoid; qu, quadrate. Photo credit: Museum of Comparative Zoology, Harvard University

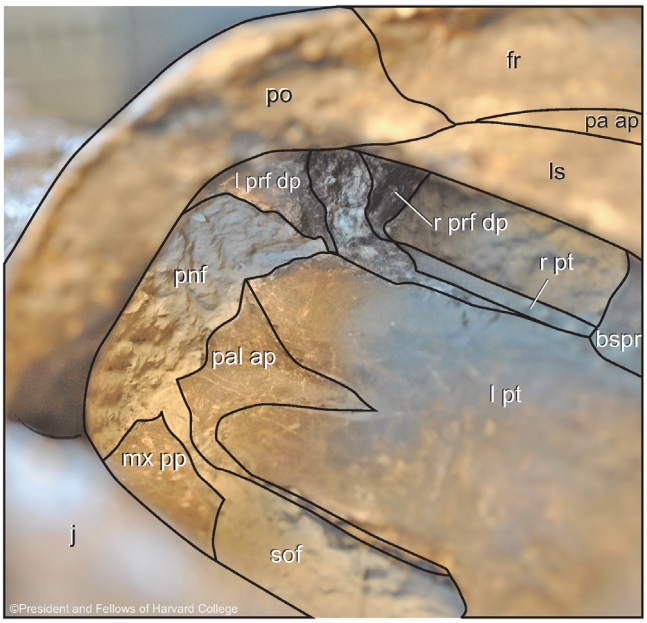

FIGURE 7 Photograph with superimposed line interpretation of the prefrontal pillar region of *Macrospondylus bollensis* (MCZ VPRA-1063) in oblique view through the left supratemporal fenestra. bspr, basisphenoid rostrum; fr, frontal; j, jugal; l prf dp, descending process of left prefrontal; l pt, left pterygoid; ls, laterosphenoid; mx pp, palatal process of maxilla; pal ap, ascending process of palatine; pa ap, anterolateral process of parietal; pnf, postnasal fenestra; po, postorbital; r prf dp, descending process of right prefrontal; r pt, right pterygoid; sof, suborbital fenestra. Photo credit: Museum of Comparative Zoology, Harvard University

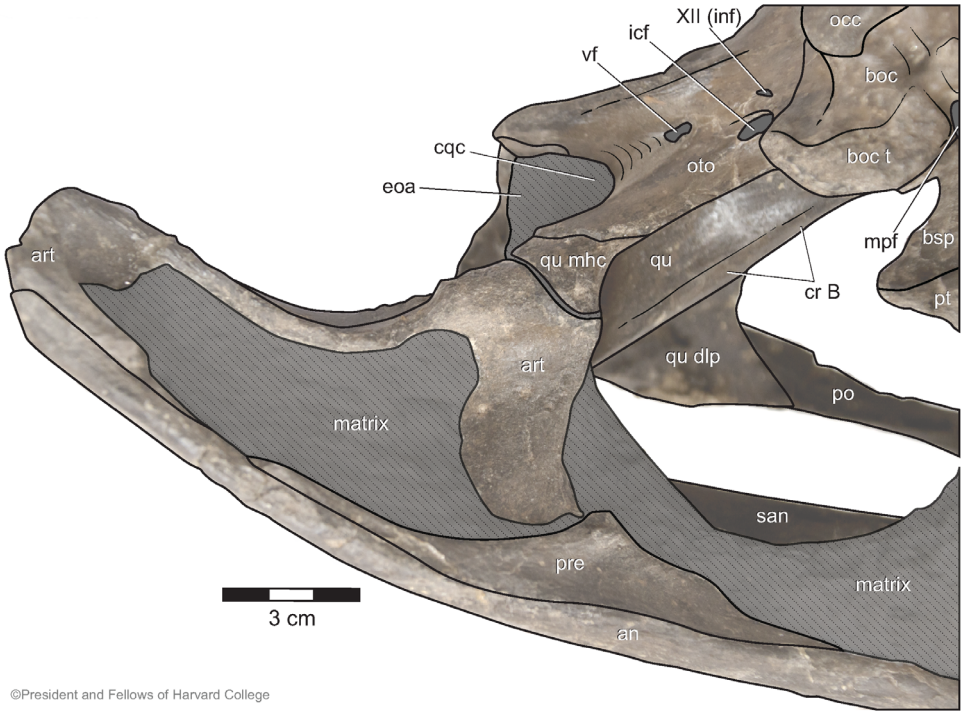

FIGURE 8 Photograph with superimposed line interpretation of the medial surface of the mandible and posteroinferior surface of the occipital region of *Macrospondylus bollensis* (MCZ VPRA-1063) in oblique inferior view. Dotted diagonal lines indicate remaining matrix. an, angular; art, articular; boc, basioccipital; bsp, basisphenoid; cqc, cranioquadrate canal; cr B, crest B; eoa, external otic aperture; icf, internal carotid foramen; mpf, median pharyngeal foramen; occ, occipital condyle; oto, otoccipital; po, postorbital; pre, prearticular; pt, pterygoid; qu, quadrate; qu dlp, dorsolateral process of quadrate; qu mhc, medial hemicondyle of quadrate; san, surangular; vf, vagus foramen; XII (inf), inferior hypoglossal foramen. Photo credit: Museum of Comparative Zoology, Harvard University

3.1 | Major openings

Antorbital fenestra: Both antorbital fenestrae are preserved (Figures 1–3). Like other teleosauroids that retain an antorbital fenestra, it is a small, obliquely oriented, ovate opening with no antorbital fossa. It is much smaller than the orbit (<25% of its length). The medial, posterior, and a small part of the lateral borders are formed by the lacrimal. The anterior border is formed by the maxilla and the lateral border is formed by the anterior process of the jugal.

Orbit: The orbits are moderately sized and circular in both dorsal and lateral views (i.e., are oriented dorsolaterally, rather than dorsally; Figures 1–3). The prefrontal and frontal form the medial border. The lacrimal makes up the anterior border. Posteriorly the orbit is bordered by the frontal and postorbital. The postorbital and lacrimal are in contact along the lateral border, excluding the jugal from the orbital margin.

Supratemporal fenestra: The supratemporal fenestrae are large and approximately 1.25 times anteroposteriorly longer (as measured to the posterior limit of the supratemporal fossa) than mediolaterally wide (Figure 1). This elongation is more pronounced than the nearly square fenestrae of *Teleosaurus cadomensis* (MNHN AC 8746; Jouve, 2009), but less dramatic than some other teleosauroids like machimosaurines (e.g., *Lemmysuchus* ("*Steneosaurus*") *obtusidens* [NHMUK PV R 3168]), where the fenestrae may be more than twice as long as wide. The anterior margin is inclined slightly anterolaterally, similar to *Teleosaurus* (see Jouve, 2009), *Mystriosaurus laurillardi* ("*Steneosaurus brevior*") (NHMUK PV OR 14781; Sachs et al., 2019), and *Platysuchus multiscrobiculatus* (SMNS 9930), giving the fenestra a trapezoid shape in dorsal view (longer laterally than medially). This differs from the posterolaterally inclined anterior margin (and parallelogram shape) found in many other teleosauroids (e.g., *Lemmysuchus obtusidens* [NHMUK PV R 3168]; *Charitomenosuchus* ("*Steneosaurus*") *leedsi* [NHMUK PV R 3320]; *Machimosaurus* [SMNS 91415]).

The anterior margin is formed by approximately equal contributions from the frontal and postorbital. The medial margin is formed by the frontal (~25%) and parietal (~75%). The lateral margin is formed primarily by the postorbital, with the squamosal forming the posterior 20%. The posterior margin is a raised crest formed by approximately equal contributions from the parietal and squamosal. The lateral margin is ventrally situated relative to the medial margin as in other thalattosuchians,

such that the supratemporal fenestrae open somewhat dorsolaterally (Figure 2). The supratemporal fossa is well developed posteriorly and medially.

Infratemporal fenestra: The infratemporal fenestrae are elongate and oval-shaped, approximately four times longer than tall (Figure 2). They open laterally such that they are largely obscured by the lateral temporal bar in dorsal view. The postorbital forms the anterior border and half of the dorsal border of the fenestra. The remainder of the posterior half of the dorsal border consists of approximately equal contributions from the squamosal and quadrate. The quadratojugal forms the posterior margin and a small part of the ventral margin of the fenestra. The jugal makes up the remainder of the ventral margin.

Temporo-orbital canal: The temporo-orbital canal is located in the posterior wall of the supratemporal fossa and is visible in dorsal and lateral views (Figures 1, 2, and 5). The opening is an elongate oval oriented mediolaterally. The parietal makes up the dorsal half of the medial border and most of the dorsal border. The prootic makes up the inferior half of the medial border and most of the ventral border. The squamosal forms the lateral border and small parts of both the dorsal and ventral borders. A small inferomedial process of the squamosal meets the prootic along the ventral margin of the temporo-orbital foramen excluding the quadrate from its margin. The temporo-orbital foramen opens into a shallow groove, which extends anteromedially along the prootic-parietal suture.

Posttemporal fenestra: The posttemporal fenestrae are narrow slot-like openings visible in occipital view (Figure 4). They are elongated mediolaterally, opening along the contact between the dorsal margin of the parietal and supraoccipital. The parietal makes up the superior and medial borders. The inferior border is formed by the supraoccipital. The otoccipital makes a small contribution to the inferolateral border.

Foramen magnum: The foramen magnum is ovoid, slightly wider than tall (Figure 4). The otoccipitals form the dorsal, lateral, and a small part of the ventral margin of the foramen. The basioccipital forms the remainder of the ventral border.

Cranioquadrate canal: The cranioquadrate canal lies close to the lateral border of the occipital surface as in other thalattosuchians. It is fully enclosed laterally by a short contact between the otoccipital and quadrate, separating it from the external otic aperture (Figure 4). The otoccipital forms its ventral and medial borders, as well as the inferior half of the lateral border and medial half of the dorsal border. The quadrate makes up the dorsal half of the lateral border and the squamosal makes up the lateral half of the dorsal border. Neither canal is fully prepared, so additional details of this opening are unclear.

External otic aperture: The external otic aperture opens posterolaterally (Figures 2 and 4). The quadrate forms its ventral, anterior, and dorsal margins, as well as the dorsal-most part of the posterior margin. The otoccipital forms the remainder of the posterior margin. Its posterior margin is medially inset relative to the dorsal and anterior (and to a lesser extent, inferior) margins (Figure 4). Among crocodylomorphs, thalattosuchians have a unique morphology of the otic region, hindering inferences regarding soft tissue structures of the external ear (see Montefeltro, Andrade, & Larsson, 2016 for detailed discussion).

Suborbital fenestra: Only the dorsal rims of the suborbital fenestrae are visible since the palatal surface of the specimen is not prepared (Figures 1, 4, and 7). They are teardrop shaped with the apex oriented anteriorly. They are slightly longer than wide, with a length approximately equal to that of the orbit. The anterior margin of the suborbital fenestra, located close to the midpoint of the orbit, lies far posterior to the anterior margin of the orbit. The anterior margin of the suborbital fenestra terminating posterior to the anterior margin of the orbit is common among teleosauroids, shared with *Indosinosuchus potamosiamensis* (see Martin et al., 2019), *Mycterosuchus nasatus* (NHMUK PV R 2617), *Machimosaurus buffetauti* (SMNS 91415), and *Neosteneosaurus edwardsi* ("*Steneosaurus durobrivensis*"; NHMUK PV R 2865). This differs from the condition in *Teleosaurus* (see Jouve, 2009) and *Charitomenosuchus leedsi* (NHMUK PV R 3806) where the anterior margin of the suborbital fenestra slightly exceeds the anterior margin of the orbit. The palatine and palatal process of the maxilla meet at the anterior apex of the suborbital fenestra. The palatine forms the medial border, the maxilla the anterior half of the lateral border, the ectopterygoid the posterior half of the lateral border, and the pterygoid the posterior border.

External mandibular fenestra: The external mandibular fenestra is large and anteroposteriorly elongate (approximately twice the length of the orbit). It is bounded anteriorly by the dentary. The surangular forms the dorsal, posterior, and slightly less than half of the ventral margin (Figure 2). The remainder of the ventral margin is formed by the angular.

3.2 | Bones of the skull

Maxilla: The posterior portion of both the left and right maxillae are preserved, forming the majority of an elongate, slender rostrum (Figures 1–3). Ornamentation of

the maxillae is subdued, limited to anteroposteriorly aligned grooves. Anteriorly the maxillae meet at the dorsal midline, separating the anterior process of the nasals from the premaxillae as in all other teleosauroids. The posteroventral process of the maxilla extends ventral to the orbit, terminating approximately ¾ of the way to the posterior border. Posteriorly and ventrally, the maxilla contacts the anterior process of the jugal in a long, anteromedially inclined suture. The maxilla forms the anterior border of the antorbital fenestra, but appears to be excluded from the lateral border by the anterior process of the jugal. However, the sutures are somewhat unclear in this region. More medially, the maxilla has a short contact with the anterior process of the lacrimal (anterior and medial to the antorbital fenestra), and an elongate anteromedially oriented contact with the nasal. While the palatal surface has not been prepared, the palatal process of the maxilla is visible through the orbit. The palatal process contacts the jugal posterolaterally and the palatine medially. It has a short suture with the ectopterygoid along the lateral margin of the suborbital fenestra of which the palatal process of the maxilla forms approximately the anterior half. At least 12 alveoli are preserved on the left and 13 on the right side. Westphal (1962) reports around 30 maxillary teeth in *Macrospondylus bollensis*, so likely more than half of the maxillary alveoli are missing anteriorly.

Nasal: The paired nasals are quadrilateral and taper sharply anteriorly between the maxillae (Figures 1–3). They are weakly ornamented with slight anteroposteriorly elongate grooves, similar to the maxillae. The posterior processes of the right and left nasal are separated by a wedge-like anterior process of the frontal, with the midline nasal suture terminating posteriorly at approximately the level of the anterior margin of the orbit. In the posterior region, this midline suture deepens to a distinct groove. This groove is more pronounced in some other specimens of *Macrospondylus bollensis* (e.g., SMNS 15951b). A groove (or "midline trench" sensu Johnson, Young, & Brusatte, 2019) is common in many other teleosauroids (e.g., *Plagiophthalmosuchus* ("*Steneosaurus*") *gracilirostris* [NHMUK PV R 757]; *Platysuchus* [SMNS 9930]) and basal metriorhynchoids (e.g., *Pelagosaurus* [NHMUK PV OR 32599]*; Opisuchus meieri* [see Aiglstorfer et al., 2020]). A broader depression in this area is common in many metriorhynchids (e.g., *Cricosaurus suevicus* [SMNS 9808]; "*Metriorhynchus*" *brachyrhynchus* [NHMUK PV R 3700]). Posteriorly and laterally, the nasal contacts the prefrontal and lacrimal, while anteriorly and laterally, it contacts the maxilla. The nasal does not participate in the margin of the antorbital fenestra. Anteriorly, the nasals terminate around the 7–8th maxillary tooth from the posterior end of the toothrow, and thus make up a small portion of the rostrum as in most teleosauroids.

Lacrimal: The lacrimal is subtriangular, forming much of the anterior and lateral border of the orbit (Figures 1–3). It is faintly ornamented with small pits. It forms the posterior and medial borders of the antorbital fenestra as in many teleosauroids that retain an antorbital fenestra (e.g., *Indosinosuchus* [PRC-11; Martin et al., 2019)]; *Teleosaurus cadomensis* [see Jouve, 2009]; *Yvridiosuchus* ("*Steneosaurus*") *boutilieri* [OUMNH J1401; Johnson et al., 2019]). The posterior process of the lacrimal is especially elongate, meeting, or nearly meeting, an elongate anteroventral process of the postorbital along the lateral border of the orbit as in *Platysuchus multiscrobiculatus* (SMNS 9930) and the Chinese teleosauroid (IVPP V 10098). Whether the lacrimal and postorbital actually articulate along the orbital margin is variable in *Macrospondylus bollensis* specimens (pers. obs.; Mueller-Töwe, 2006), but in specimens where they do not meet, they are very close. Laterally, the lacrimal has a gently curved, elongate suture with the jugal, which ends anteriorly at the posterolateral edge of the antorbital fenestra. Medially, the lacrimal meets with the prefrontal in the anteromedial region of the orbital margin. The prefrontal-lacrimal suture extends anteriorly and is continuous with the lacrimal-nasal suture. The anterior process of the lacrimal extends anteriorly beyond the antorbital fenestra, excluding the nasal from participation in the border of the fenestra. The orbital surface of the lacrimal broadens medially where it meets with the orbital surface of the prefrontal.

Jugal: The jugal is a triradiate bone with elongate anterior and posterior processes and a short dorsomedial process. In MCZ VPRA-1063 the right and left jugals are partially preserved, both lacking much of their posterior processes (Figures 1, 2, and 5). The outer surface of the jugal is weakly ornamented with anteroposteriorly oriented shallow grooves. Anteriorly and laterally, the jugal articulates with the maxilla in an elongate anteromedially sloping suture. The jugal appears to be excluded (or nearly so) from the lateral border of the orbit by the thin posterior process of the lacrimal meeting with the anteroventral process of the postorbital. The anterior process of the jugal greatly exceeds the anterior margin of the orbit, reaching a point just anterior to the anterior margin of the antorbital fenestra. The jugal superficially contributes to the lateroventral border of the antorbital fenestra, but given the gracility of this process, it seems likely that it is merely overlying the maxilla, which forms this border deep to the jugal.

The jugal is widely exposed lateral to the orbit, though posteriorly, the descending process of the postorbital strongly overlaps it laterally such that in lateral view

it is completely covered between the anterior and posterior processes as in most teleosauroids. Just dorsal to its suture with the maxilla, lateral to the orbit, the jugal bears a shallow, but distinct, elongate groove paralleling the suture. This groove is more evident on other specimens of *Macrospondylus bollensis*, and it is unclear whether this represents individual variation, or differences in specimen preparation. Superiorly, the jugal articulates with, and is broadly overlapped by, the postorbital. The jugal forms the ventromedial portion of the wide postorbital bar, articulating medially with the ectopterygoid and the palatal process of the maxilla. The jugal is just excluded from the lateral border of the suborbital fenestra by a contact between the anterior process of the ectopterygoid and the palatal process of the maxilla.

The posterior process of the jugal is broken and largely reconstructed on both sides. However, a short portion of the lower temporal bar is preserved on each side. The posterior process is dorsoventrally flattened and roughly rectangular in cross section (being approximately twice as wide as tall). Posteriorly, a small part of its articulation with the quadratojugal is preserved on the right side only. This, along with the preserved quadratojugals, demonstrates that the jugal would not have reached the posterior edge of the infratemporal fenestra (i.e., the jugal/quadratojugal suture lies along the ventral border, rather than at the posteroventral corner as in most crocodyliforms).

Prefrontal: The prefrontal is a small triangular bone in dorsal view forming the anteromedial and slightly less than half of the medial border of the orbit (Figure 1). The external surface is ornamented with a series of very faint pits similar to the lacrimal. The posterior end of the prefrontal is located just anterior to the anteroposterior midpoint of the orbit. Anteriorly, the prefrontal is much shorter than the lacrimal, ending posterior to the edge of the antorbital fenestra. The prefrontal contacts the frontal posteriorly and medially, the nasal medially, and the lacrimal anteriorly and laterally. It has a broad orbital surface (orbital lamina) that tapers ventrally and medially as the prefrontal pillar. The prefrontal pillar is transversely broad dorsally, and tapers ventrally where it has a narrow contact with the dorsal process of the pterygoid (Figures 3 and 7). The articulation of the descending process of the prefrontal with the palate is variable among thalattosuchians. Among metriorhynchoids, the descending process of the prefrontal fails to reach the palate in *Pelagosaurus* (NHMUK PV OR 32599), whereas it contacts, or very nearly contacts, the ascending process of the palatine and/or vomer in *Zoneait nargorum* (UOMNH F39539; Wilberg, 2015a), and robustly contacts the ascending process of the palatine in metriorhynchids (e.g., *Cricosaurus araucanensis*; Fernández & Herrera, 2009). The ventral extent of the prefrontal pillar is poorly known among teleosauroids, likely due to the prevalence of dorsoventral compression during fossilization. Jouve (2009) reported that the descending process of the prefrontal articulated with a fragment of bone identified as palatine in *Teleosaurus cadomensis*. The descending process of the prefrontal clearly contacts the palate in *Proexochokefalos* ("*Steneosaurus*") *heberti* (MNHN 1890-13), however it is unclear whether the bone it contacts is palatine or pterygoid.

Frontal: The unpaired frontal is cruciform in dorsal view, articulating with the prefrontals and nasals anteriorly, the postorbitals laterally, and the parietal and laterosphenoid posteriorly (Figure 1). The dorsal lamina of the frontal is ornamented by a series of ovate pits, radiating from a point just anterior to the interfenestral bar. These pits appear shallower and less pronounced on this specimen than on others of *Macrospondylus bollensis* (e.g., NHMUK PV OR 14436; GPIT Re 1193/1), but this could be due to differences in preservation and/or preparation. The frontal is broad between the orbits, and forms the posterior half of the medial border of the orbit and slightly less than half of the posterior border. Its anterior process forms a shallow V-shape, separating the posterior processes of the nasals and slightly exceeding the anterior margin of the orbit. This short, broad anterior process is shared with a number of other teleosauroids (e.g., *Platysuchus* [SMNS 9930]; *Neosteneosaurus edwardsi* [NHMUK PV R 2865]), but differs from other forms such as *Charitomenosuchus leedsi* (NHMUK PV R 3320) and *Indosinosuchus* (PRC-11), which have a narrower, more sharply tapering process. The anterior process ends well posterior to the anterior margin of the prefrontals, differing from taxa such as *Indosinosuchus*, in which the anterior process of the frontal reaches the anterior margin of the prefrontal. Ventrally, the descending processes of the frontal form the lateral walls of a shallow midline olfactory groove.

The lateral process of the frontal articulates with the postorbital along the posterior margin of the orbit, forming a narrow bar separating the orbit from the supratemporal fenestra. The suture with the postorbital is irregular, but more or less directed anteroposteriorly, similar to other teleosauroids, but differing from the distinct V-shaped suture found in metriorhynchoids.

Posteriorly, the frontal articulates with the parietal and laterosphenoid, forming the anteromedial border of the supratemporal fenestra and contributing to the supratemporal fossa (Figures 1 and 5). The lateral processes form an angle with the posterior process of just over 90°. This feature is shared with some teleosauroids such as *Platysuchus multiscrobiculatus* (SMNS 9930),

Indosinosuchus potamosiamensis (PRC-11), the Chinese teleosauroid (IVPP V 10098), and *Mystriosaurus laurillardi* (NHMUK PV OR 14781). However, it differs from the posteriorly inclined lateral processes of machimosaurines and *Charitomenosuchus leedsi* (NHMUK PV R 3320). The frontal forms approximately the anterior third of the interfenestral bar and contributes to the anteromedial portion of the supratemporal fossa. Within the supratemporal fossa, the frontal has a short contact with the postorbital and laterosphenoid and an elongate contact with the thin anterolateral processes of the parietal (also present in the Chinese teleosauroid [IVPP V 10098]; *Platysuchus* [UH 1]. This differs from some other teleosauroids like *Teleosaurus* (MNHN AC 8746; Jouve, 2009) in which the anterolateral process of the parietal contacts the postorbital. The full phylogenetic distribution of this character among teleosauroids is difficult to discern as this region is often highly fractured or the sutures are indistinct.

Parietal: The parietal is a single fused element as in other derived crocodylomorphs (e.g., *Sphenosuchus*, *Junggarsuchus*, *Macelognathus*, and *Almadasuchus*; Leardi, Pol, & Clark, 2020) and crocodyliforms. The bone is T-shaped in dorsal view (Figure 1). The anterior process of the parietal forms the posterior two thirds of the interfenestral bar and articulates with the frontal anteriorly and the laterosphenoids and prootics laterally. Long, slender anterolateral processes extend along the lateral margin of the posterior process of the frontal. A short contact between the frontal and laterosphenoids prevents contact between the anterolateral process of the parietal and the postorbital within the supratemporal fossa. The lateral suture between the anterior process of the parietal and the dorsal margin of the laterosphenoid and prootic does not form a straight line. Rather, the suture between the parietal and laterosphenoid lies ventral to that between the parietal and prootic (Figures 1, 2, and 5). A narrow, but low, sagittal crest spans the length of the intertemporal bar on both the frontal and parietal.

The lateral processes of the parietal articulate with the prootics anterolaterally, the squamosals laterally and the otoccipitals posteriorly. The anterior margin of the distal end of the lateral process forms the dorsal and medial borders of the temporo-orbital canal. The suture with the squamosal begins near the dorsolateral corner of the temporo-orbital canal and is inclined posterolaterally. This suture lies almost entirely within the supratemporal fossa. The lateral process of the parietal forms approximately half of the posterior border of the broad supratemporal fossa which terminates at a narrow ridge extending along the dorsolateral surface of the parietal and posteromedial surface of the squamosal. However, the dorsal-most portion of this ridge is not preserved.

Where the anterior and lateral processes meet, there is a small triangular "parietal table" (sensu Brusatte et al., 2016). In other specimens of *Macrospondylus bollensis* (e.g., SMNS 15951b), this is typically slightly larger and flatter, bearing scattered pits, similar to the ornamentation of the frontal. The dorsal surface appears irregular in MCZ VPRA-1063, suggesting this area has been damaged. This portion of the parietal articulates posteroventrally with the supraoccipital, excluding it from the dorsal surface of the skull as in other thalattosuchians. The narrow occipital surface of the parietal forms the superior margin of the slit-like posttemporal fenestrae, located along this parietal-supraoccipital suture (Figure 4).

Postorbital: This is a triradiate bone with a broad anteroventral process, a short narrow medial process, and an elongate narrow posterior process. In MCZ VPRA-1063 both postorbitals are completely preserved and lack ornamentation (Figures 1–3, and 5). The postorbital articulates with the jugal and lacrimal anteriorly, the frontal and laterosphenoid medially, and the squamosal and quadrate posteriorly. It forms the posterolateral margin of the orbit. The broad anteroventral process overlaps the ascending process of the jugal laterally, forming the entire lateral surface of the broad postorbital bar. Anteromedially, this process forms a short suture with the lacrimal, excluding the jugal from the lateral margin of the orbit. Posteriorly, the postorbital bar is slightly inset, with a shallow depression extending anteriorly from the anterior margin of the infratemporal fenestra.

The medial process of the postorbital meets the lateral process of the frontal in an anteroposteriorly directed suture near the midpoint of the posterior margin of the orbit. Posteriorly, this medial process forms the lateral half of the anterior border of the supratemporal fenestra. It contributes slightly to the anteromedial corner of the supratemporal fossa, where it contacts the laterosphenoid. Along the ventral surface, the medial process of the postorbital contacts the capitate process of the laterosphenoid.

The posterior process of the postorbital articulates with the squamosal posteriorly and the quadrate posteroventrally. The articulation with the anterior process of the squamosal is inclined from anteroventral to posterodorsal, resulting in the dorsal surface of the posterior process being longer than the ventral surface. The posterior process is considerably longer than the anterior process of the squamosal as in most thalattosuchians, forming approximately 75% of the lateral border of the supratemporal fenestra. In lateral view, the postorbital makes up approximately half of the dorsal border of the infratemporal fenestra. An anteriorly tapering dorsolateral process of the quadrate articulates with the ventral surface of the posterior process of the postorbital.

Squamosal: Both squamosals are nearly complete. The squamosal is an L-shaped element, with anterior and

medial processes (Figures 1, 2, 4, and 5). It contacts the postorbital anteriorly, the parietal and prootic medially, the quadrate ventrally, and the paroccipital process of the otoccipital posteriorly. The anterior process underlaps the posterior process of the postorbital and forms the posterior 25% of the lateral margin of the supratemporal fenestra and approximately 25% of the dorsal border of the infratemporal fenestra. The ventral surface of the anterior process of the squamosal articulates with the dorsolateral process of the quadrate. The dorsolateral process of the quadrate sends a thin lamina of bone along the dorsal margin of the external otic aperture, excluding the squamosal from participation in this opening. Immediately posterior to the external otic aperture lies a distinct, dorsally directed notch along the ventral margin of the squamosal. A similar notch is present in the Chinese teleosauroid (IVPP V 10098), *Indosinosuchus* (PRC-11), and *Platysuchus multiscrobiculatus* (SMNS 9930). A much less pronounced notch in the squamosal just posterior to the external otic aperture is present in other teleosauroids (e.g., *Proexochokefalos heberti* [MNHN 1890-13]; *Machimosaurus buffetauti* [SMNS 91415]). The squamosal has no contact with the quadrate posterior to the external otic aperture.

The medial process of the squamosal forms approximately half of the posterior margin of the supratemporal fenestra. Its anterior surface is inclined posterodorsally, contributing to the posterolateral region of the supratemporal fossa. Within the supratemporal fossa, the squamosal contacts the prootic ventromedially and the parietal dorsomedially. Interposed between these bones lies the temporo-orbital foramen. The squamosal forms the lateral margin of the temporo-orbital canal. The contact between the squamosal and prootic excludes the quadrate from the external opening of the temporo-orbital canal. Ventrally, the medial process of the squamosal is sutured with the dorsal surface of the quadrate.

The posterolateral region of the squamosal is developed into an elongate ventrolaterally directed squamosal fossa (complete on the left side; Figures 1 and 4). A posterolaterally directed flat or concave surface on this region of the squamosal is common among thalattosuchians and is often referred to as the "squamosal flat surface" (e.g., Martin et al., 2019; Martin & Vincent, 2013; Parrilla-Bel et al., 2013; Pol & Gasparini, 2009; Young et al., 2013). However, the morphology of this surface differs between taxa, typically being rounder and more dorsally positioned in metriorhynchids. The elongate squamosal fossa of MCZ VPRA-1063 is reminiscent of (but likely not homologous with) a similar feature present in derived non-crocodyliform crocodylomorphs such as *Junggarsuchus* (IVPP V 14010) and *Almadasuchus* (Leardi et al., 2020; Pol et al., 2013). The medial margin of this squamosal fossa forms an interlocking suture with the paroccipital process of the otoccipital, overhanging the lateral third of the cranioquadrate canal and contributing slightly to its dorsal margin.

Quadratojugal: Both quadratojugals are largely preserved and devoid of ornamentation (Figures 2, 4, and 5). The quadratojugal is a small, somewhat C-shaped bone articulating with the distal end of the jugal laterally and the quadrate medially. The right quadratojugal is more complete than the left sending a small projection anteriorly along the medial surface of the jugal to exclude the jugal from the posterior edge of the infratemporal fossa as in *Indosinosuchus* (Martin et al., 2019) and *Teleosaurus* (Jouve, 2009). The quadratojugal thus forms the posteroventral margin of the infratemporal fossa and is laterally concave in this region. Posteriorly, the quadratojugal nearly reaches the lateral quadrate hemicondyle and does not contribute to the articulation surface.

The ascending process of the quadratojugal is very short, ascending about halfway up the dorsolateral process of the quadrate. The quadratojugal fails to contact the squamosal or the postorbital and does not contribute to the dorsal margin of the infratemporal fossa. As in other known thalattosuchians, there is no evidence of a quadratojugal spine.

Quadrate: Both quadrates are well preserved in MCZ VPRA-1063 (Figures 1, 2, 4–6, and 8). However, they are in articulation with the articular bones obscuring the morphology of the condyle. The quadrate is a complex bone articulating with the quadratojugal laterally, the squamosal anterodorsally, the otoccipital posterodorsally, the prootic anteromedially, the basisphenoid and pterygoid ventromedially. The quadrate body is mediolaterally broad and anteroposteriorly short, failing to exceed the occipital condyle posteriorly. It is not visible in dorsal view, as it is obscured by the squamosal and otoccipital. The quadrate body is inclined posteroventrally, positioning the quadrate condyle slightly ventral to the occipital condyle. It articulates laterally with the small quadratojugal. Because the quadrates are preserved in articulation with the articulars, the details of the quadrate condyle are not visible. However, it appears the medial hemicondyle reaches further ventrally than the lateral one. The quadrate body lacks any subtympanic foramina (sensu Dufeau & Witmer, 2015; Montefeltro et al., 2016) or a quadrate foramen aereum as in all thalattosuchians (Herrera et al., 2018).

As in other thalattosuchians, the posterodorsal surface of the quadrate body is strongly overlapped by a ventrolateral flange of the otoccipital, covering about the medial 75% of its width. The dorsolateral process of the quadrate has a broad articulation with the squamosal and a short articulation with the posterior process of the

postorbital. This process forms approximately the posterior 25% of dorsal border of the infratemporal fenestra. The dorsolateral process of the quadrate forms the entirety of the posterolaterally directed otic incisure (sensu Montefeltro et al., 2016), and sends a posterior otic lamina along the ventral surface of the squamosal, separating it from the external otic aperture. The posteromedial margin of this posterior otic lamina meets with the otoccipital, forming the lateral margin of the cranioquadrate canal and separating it from the otic recess. The complete separation of the cranioquadrate canal from the otic recess is variable among thalattosuchians, being completely separated in metriorhynchids (e.g., *C. araucanensis*; Herrera et al., 2018) and some teleosauroids (e.g., *Machimosaurus buffetauti* [SMNS 91415]). However, the cranioquadrate canal is reported as incompletely separated from the external otic aperture (with the ascending lamina of the otoccipital not quite reaching the otic lamina of the quadrate) in *Teleosaurus cadomensis* (Jouve, 2009), *Indosinosuchus* (Martin et al., 2019), and "*Steneosaurus*" *pictaviensis* (Herrera et al., 2018). The condition in *Pelagosaurus typus* is less clear. In NHMUK PV OR 32599, the swelling at the posterior end of the otic lamina of the quadrate just contacts an ascending lamina of the otoccipital lateral to the cranioquadrate canal on the left side, completing the separation (pers obs.; Clark, 1986; Montefeltro et al., 2016), but these bones are slightly separated on the right side. Herrera et al. (2018) report a slightly incomplete separation in SNSB-BSPG 1890 I5 (and NHMUK PV OR 32599) and note that the connection between the quadrate and otoccipital may have been formed by cartilage in life.

The ventral surface of the quadrate body is smooth and marked by an elongate anteromedially oriented crest (Crest B of Iordansky, 1964, 1973) dividing the surface into two shallow fossae. The apex of this crest is well developed but rounded, similar to most thalattosuchians. This differs from that reported in another specimen of *Macrospondylus bollensis* (SNSB-BSPG 1984 I258; Herrera et al., 2018) in which the crest has a sharp, narrow apex. Ventromedially, the quadrate contacts the basisphenoid and the quadrate process of the pterygoid, but is separated from the basioccipital by narrow wings of the basisphenoid. A contact between the quadrate and basioccipital is present in metriorhynchoids (e.g., *Opisuchus* [see Aiglstorfer et al., 2020]; *Cricosaurus araucanensis* [see Herrera et al., 2018]; *Purranisaurus potens* [see Herrera et al., 2015]). However, a contact between these bones is absent in many teleosauroids (e.g., *Teleosaurus cadomensis* [see Jouve, 2009]; *Indosinosuchus* [PRC-8; Martin et al., 2019]; *Charitomenosuchus leedsi* [NHMUK PV R 3320]), though the full phylogenetic distribution of this character is unclear as many specimens are heavily fractured in this region. A contact between the quadrate and basioccipital is reportedly present in the basal-most teleosauroid *Plagiophthalmosuchus* (Brusatte et al., 2016), and basal-most metriorhynchoid *Pelagosaurus typus* (Herrera et al., 2018) which would suggest this configuration is ancestral for Thalattosuchia. However, in NHMUK PV OR 32599 (an exquisitely preserved acid-prepared *Pelagosaurus* skull), a thin flange of basisphenoid seems to extend lateral to the lateral Eustachian foramen, separating the quadrate from the basal tuber. The specimen of *Plagiophthalmosuchus*, reported on by Brusatte et al. (2016) is not particularly well preserved in this area, making the identification of a potentially thin slip of basisphenoid difficult. Thus, the distribution of this character among Thalattosuchia requires further investigation.

The dorsal primary head of the quadrate broadly contacts the lateral wall of the braincase. Posteromedially it has a broad contact with the otoccipital. Anteromedially, it is sutured to the ventral margin of the medial process of the squamosal and the ventral margin of the prootic, contributing to the posteroventral wall of the supratemporal fossa. A narrow contact between the squamosal and prootic excludes the quadrate from the external opening of the temporo-orbital canal. The exclusion of the quadrate from the temporo-orbital opening is common among metriorhynchoids (e.g., *Pelagosaurus typus*, *Cricosaurus araucanensis*, *Opisuchus meieri*; Aiglstorfer et al., 2020), but it participates slightly in the ventral margin in most teleosauroids (e.g., *Teleosaurus cadomensis* [see Jouve, 2009]; *Machimosaurus buffetauti* [SMNS 91415]; *Indosinosuchus* [see Martin et al., 2019]). However, this region is not typically described in detail (and may be difficult to interpret depending on preservation) in many morphological descriptions of teleosauroids. A similar contact excluding the quadrate from the margin of the temporo-orbital foramen is present in the Chinese teleosauroid (IVPP V 10098).

Ventromedially, the dorsal primary head projects a short contact with the pterygoid and an elongate, finger-like orbital process. As in other thalattosuchians (e.g., *Pelagosaurus* [NHMUK PV OR 32599]; *Zoneait nargorum* [UOMNH F39539; Wilberg, 2015a]; *Cricosaurus araucanensis* [see Herrera et al., 2018]; *Purranisaurus potens* [see Herrera et al., 2015]; *Machimosaurus buffetauti* [SMNS 91415]; *Teleosaurus cadomensis* [see Jouve, 2009]), the orbital process lacks bony attachment to the pterygoid, basisphenoid, or laterosphenoid anteromedially. This elongate orbital process helps define the margin of the trigeminal fossa in which the quadrate forms the ventral, posterior, and part of the dorsal border. Along the dorsolateral surface of the orbital process, a slight depression may indicate the passage of the mandibular division of the trigeminal nerve

(V_3). The trigeminal fossa is greatly expanded posteriorly, communicating with the paratympanic sinus via a foramen similar in size to the trigeminal foramen ("Foramen 2"; Figure 5). This posterior expansion of the trigeminal fossa is shared with metriorhynchids (e.g., "*Metriorhyhchus*" cf. *westermanni* [see Fernández, Carabajal, Gasparini, & Chong, 2011]; *Cricosaurus araucanensis* [see Herrera et al., 2018]) and some teleosauroids (e.g., *Indosinosuchus* [see Martin et al., 2019]; *Machimosaurus buffetauti* [SMNS 91415]), but appears more extensive than that of more basal thalattosuchians (e.g., *Pelagosaurus* [NHMUK PV OR 32599]; *Plagiophthalmosuchus* [NHMUK PV OR 33095; Brusatte et al., 2016]).

Otoccipital: The exoccipitals and opisthothics are fused into as single otoccipital on each side. The otoccipitals make up most of the occipital surface (Figures 4 and 8). The otoccipital articulates with the supraoccipital dorsomedially, the parietal dorsally, the squamosal dorsolaterally, the quadrate laterally and ventrolaterally, and the basioccipital and basisphenoid ventromedially. The right and left otoccipital meet at a straight suture dorsal to the foramen magnum, of which the otoccipitals make up the dorsal, lateral, and a small part of the ventral margin. The articulation with the supraoccipital gently curves from ventromedial to dorsolateral, ending at a small occipital tuberosity where it meets the parietal. This occipital tuberosity appears to make a very slight contribution to the ventrolateral margin of the slit-like posttemporal fenestra. Small occipital tuberosities on the otoccipital (with a minor contribution from the supraoccipital) are common among teleosauroids (e.g., *Plagiophthalmosuchus* cf. *gracilirostris* [NHMUK PV OR 33095; Brusatte et al., 2016]; *Teleosaurus cadomensis* [see Jouve, 2009]; *Deslongchampsina* ("*Steneosaurus*") *larteti* [see Johnson et al., 2019]). They are larger and better developed in *Proexochokefalos heberti* (MNHN 1890-13; Johnson et al., 2020a, 2020b), but are still smaller than those of most dyrosaurs (e.g., *Rhabdognathus aslerensis* [AMNH FARB 33354]; *Dyrosaurus phosphaticus* [MNHN ALG 2]).

The paroccipital processes are well developed and posteroventrally inclined. The dorsal surface is gently concave, becoming more pronounced towards the occipital tuberosities. Laterally, it interlocks with the squamosal in a U-shaped articulation, just medial to the squamosal fossa. The otoccipital is largely smooth, but posterolaterally the paroccipital process is thick and rugose, especially where it overhangs the region of the cranioquadrate canal. Laterally, the paroccipital process articulates with the otic flange of the quadrate, enclosing the cranioquadrate canal.

The ventrolateral flange of the otoccipital spreads broadly across the dorsal surface of the quadrate body in a somewhat sigmoid raised suture posteriorly (more posteriorly positioned medially and laterally). A broad ventrolateral flange is present in both protosuchids (Clark, 1994; Pol & Gasparini, 2009) and thalattosuchians, but is more expanded in thalattosuchians. This ventrolateral flange covers much of the quadrate body in occipital view. Ventromedially, the otoccipital contacts the basioccipital along the lateral and dorsolateral margins of the basal tubera and participates slightly in the dorsolateral portion of the occipital condyle. This part of the otoccipital also forms much of the posterior border of the lateral Eustachian foramen (= pharyngotympanic foramen), and has a short suture with the posterolateral flange of the basisphenoid, just lateral to the lateral Eustachian foramen (Figure 6).

The otoccipital is pierced by a number of foramina. Just lateral to the occipital condyle and approximately in line with the ventral border of the foramen magnum is a large posteriorly directed hypoglossal foramen (XII sup). Ventrolateral to this opening (located slightly superior to the dorsoventral midpoint of the occipital condyle) is another, smaller opening, oriented more posterolaterally. We interpret this opening as a second hypoglossal foramen (XII inf). Clark (1986) also interpreted a similar opening in the occipital surface of *Pelagosaurus* (NHMUK PV OR 32599) as a second hypoglossal foramen, but Brusatte et al. (2016) interpreted a small foramen in this location on a specimen of *Plagiophthalmosuchus* (NHMUK PV OR 33095) as the opening for CN IX. Unfortunately, the resolution of our CT data is insufficient to trace this canal and verify its identity.

Further ventrolateral to the second hypoglossal opening, approximately in line with the dorsoventral midpoint of the occipital condyle, lies the opening for the internal carotid artery. It is large, dorsoventrally elongate, and opens ventrolaterally, very close to the ventral border of the otoccipital in occipital view. A ventrolateral or posteroventrally directed internal carotid foramen is common among teleosauroids, but differs from the posteriorly directed foramen of metriorhynchoids (Herrera et al., 2018). The carotid foramen is enlarged as in all thalattosuchians (Brusatte et al., 2016; Herrera et al., 2018; Wilberg, 2015a), but is not as hypertrophied as that of metriorhynchids (Fernández et al., 2011; Herrera et al., 2018).

Another large foramen, interpreted as the vagus foramen, is positioned more laterally on the ventrolateral portion of the paroccipital process. This foramen is mediolaterally elongate and bilobate. This foramen would have transmitted cranial nerves IX-XI and associated vasculature. It is located quite lateral relative to the hypoglossal and internal carotid foramina, and positioned dorsoventrally between the two. This lateral position of the vagus foramen is common among

teleosauroids, but differs from the position in metriorhynchids, which is closer to the internal carotid foramen (Brusatte et al., 2016). The bilobate shape suggests the foramen may have been divided into two openings more deeply, but sediment infilling and low CT scan resolution prevents confirmation of this. A foramen for the glossopharyngeal (CN IX), separated from that for the vagus and accessory nerves, seems variable among thalattosuchians. Among teleosauroids, they are separate in *Teleosaurus cadomensis* (see Jouve, 2009) and potentially *Machimosaurus buffetauti* (SMNS 91415; though this area is not well preserved), but appear confluent in *Plagiophthalmosuchus* cf. *gracilirostris* (see Brusatte et al., 2016 – assuming the foramen near the internal carotid they identified as transmitting CN IX is actually a second hypoglossal foramen) and *Indosinosuchus* (PRC-8; Martin et al., 2019). Two separate foramina are present in some metriorhynchids (e.g., *Cricosaurus rauhuti* SNSB-BSPG 1973 I195; *Thalattosuchus* ("*Metriorhynchus*") *superciliosus* [NHMUK PV R 11999]; *Cricosaurus araucanensis* [see Herrera et al., 2018]), but not others (e.g., *Dakosaurus andiniensis* [see Pol & Gasparini, 2009; Herrera & Vennari, 2015]; *Torvoneustes coryphaeus* [see Young et al., 2013]). Further confounding the issue is the dearth of well-preserved occipital surfaces among thalattosuchians.

The cranioquadrate canal is positioned quite laterally on the occiput, along the lateral edge of the otoccipital as in other thalattosuchians (Clark, 1994; Herrera et al., 2018). Both cranioquadrate canals are filled with sediment, preventing detailed description. However, the right is somewhat more prepared, exposing the lateral margin. The otoccipital forms the medial margin, the medial two thirds of the dorsal margin, the inferior margin, and the inferior half of the lateral margin of the opening.

Supraoccipital: The single supraoccipital forms the superomedial portion of the occipital surface (Figures 1 and 4). It does not contribute to the dorsal surface of the skull, but is partly visible in dorsal view between the parietal and otoccipitals. It articulates dorsally with the parietal and inferiorly and laterally with the otoccipitals. In occipital view, it is roughly trapezoidal, broader dorsally than ventrally, and wider than tall. It bears a strongly raised midline nuchal crest, subdividing the overall concave surface into two fossae. This raised crest offsets the superior and inferior borders dorsally, giving each border a gently curved W-shape. The slight W-shape of the supraoccipital in occipital view is shared with the Chinese teleosauroid (IVPP V 10098), but differs greatly from the dorsoventrally tall shape of some teleosauroids (e.g., *Lemmysuchus obtusidens* [NHMUK PV R 3186; Johnson et al., 2017]; *Machimosaurus buffetauti* [SMNS 91415]; *Proexochokefalos heberti* [MNHN 1890-13]). Along the lateral edge of the dorsal border, the supraoccipital forms the ventral border of the posttemporal fenestrae.

Laterosphenoid: Both laterosphenoids are well preserved (Figures 1, 2, and 5). The laterosphenoid is anteroposteriorly elongate, dorsoventrally taller posteriorly and narrowing anteriorly. Dorsally it articulates with the parietal in a long, relatively straight suture. Anteromedially, it has a short articulation with the frontal within the supratemporal fossa. Ventral and lateral to this laterosphenoid-frontal suture, a slender capitate process extends laterally, articulating with the ventral surface of the medial process of the postorbital. Extending posteriorly from this articulation with the postorbital is a pronounced longitudinal crest of the laterosphenoid, forming the lateral margin of the anterior portion of the supratemporal fossa. The surface of the laterosphenoid ventral to this crest is oriented ventrolaterally.

Ventrally, the laterosphenoid has a long, gently curving contact with the basisphenoid rostrum, inclined from anterodorsal to posteroventral. Posteriorly, this contact with the basisphenoid passes deep to the anterior tip of the orbital process of the quadrate. Just posterior to the contact with the basisphenoid rostrum and in line with the trigeminal foramen, the laterosphenoid is pierced by a small ovate foramen for the trochlear nerve (CN IV). Holliday and Witmer (2009) described an epipterygoid as being present in thalattosuchians based on CT scans of a specimen of *Pelagosaurus* (BRLSI M1413) and note a rugose fossa where it would have articulated in NHMUK PV OR 32599. However, in MCZ VPRA-1063 there is no evidence of an epipterygoid nor a rugose fossa where it would have articulated. Anteriorly, dorsal to its contact with the basisphenoid rostrum, the left and right laterosphenoids articulate with one another, forming the ventral border of the opening for the olfactory tract. A relatively large opening between the laterosphenoids is present just ventral to the olfactory tract for transmission of the optic nerves (CN II).

Posteriorly, the laterosphenoid contacts the prootic in two areas: within the supratemporal fossa and within the trigeminal fossa (Figure 5). Its suture with the prootic within the supratemporal fossa is raised, forming a dorsoventrally oriented crest. This raised crest is present in most thalattosuchians (e.g., *Pelagosaurus* [NHMUK PV OR 32599]; *Plagiophthalmosuchus* cf. *gracilirostris* [NHMUK PV OR 33095]; *Suchodus brachyrhynchus* [NUMHK PV R 3700]), though it appears less pronounced in juveniles and small individuals (pers. obs.). The presence of a raised crest in both *Pelagosaurus* and *Plagiophthalmosuchus* suggests it is synapomorphic for Thalattosuchia. This crest divides the posterior supratemporal fossa into a posterior and anterior fossa

interpreted as the insertions for M. adductor mandibulae externus profundus and M. pseudotemporalis superficialis, respectively (Holliday & Witmer, 2009).

Within the trigeminal fossa, the laterosphenoid articulates with an anteroventrally directed process of the prootic. This contact defines the trigeminal foramen, of which the laterosphenoid forms the anterior and a small part of the anteroventral borders. The laterosphenoid has a subtle, blunt posterior process along the anterior margin of the trigeminal foramen, dividing it into dorsal and ventral lobes, similar to *Pelagosaurus* (NHMUK PV OR 32599). Extending anteriorly from the trigeminal foramen along the surface of the laterospenoid are two distinct grooves (Figure 5). The groove originating from the anteroventral margin of the trigeminal foramen is interpreted as the groove for the ophthalmic division of the trigeminal nerve (V_1), while the more dorsally placed groove is for the maxillary division of the trigeminal (V_2). The position and orientation of these grooves are consistent with those of *Pelagosaurus* (NHMUK PV OR 32599; Holliday & Witmer, 2009). However, in MCZ VPRA-1063 the groove for V_1 is not bounded dorsally by a distinct crest as in *Pelagosaurus*, and more closely resembles the shallow groove of *T. cadomensis* (see Jouve, 2009) and a different specimen of *Macrospondylus bollensis* (SNSB-BSPG 1984 I258; Herrera et al., 2018).

Prootic: The prootic is broadly exposed in the supratemporal fossa as in all thalattosuchians and non-crocodyliform crocodylomorphs (Clark, 1986; Leardi et al., 2020; Wilberg, 2015b). The exposed surface of the prootic is subtriangular in dorsal view, contacting the laterosphenoid anteriorly, the parietal dorsally, the squamosal laterally, and the quadrate ventrally (Figures 1, 2, and 5). At its lateral-most extent, the prootic contacts a thin ventromedial process of the squamosal, excluding the quadrate from the margin of the temporo-orbital foramen. The prootic forms most of the ventral border of the temporo-orbital foramen as well as the ventral half of the medial border. The ventral-most point of the supratemporal surface of the prootic overhangs the medial margin of the trigeminal fossa.

Within the trigeminal fossa, an elongate descending process of the prootic contacts the posterior margin of the laterosphenoid (Figure 5). Thus, the prootic forms the dorsal, posterior, and much of the ventral margins of the trigeminal foramen. The descending process of the prootic separates two openings in the trigeminal fossa, the trigeminal foramen medially and a second, similarly sized foramen laterally. This peculiar morphology of the trigeminal fossa seems to be a derived feature of teleosauroids. It is lacking in metriorhynchoids (e.g., *Pelagosaurus* [NHMUK PV OR 32599]; "*Metriorhynchus*" cf. *westermanni* [see Fernández et al., 2011]; *C. araucanensis* [see Herrera et al., 2018]), and the basal-most teleosauroid *Plagiophthalmosuchus* cf. *gracilirostris* (NHMUK PV OR 33095; Brusatte et al., 2016). However, in teleosauroids in which this region is prepared and well preserved (e.g., *Proexochokefalos heberti* [MNHN 1890-13]; *Machimosaurus buffetauti* [SMNS 91415]), the same morphology is present (see discussion). A similar morphology was described by Herrera et al. (2018) in SNSB-BSPG 1984 I258.

Basisphenoid: The basisphenoid is anteroposteriorly elongate, forming much of the floor of the endocranial cavity (Figures 2, 5, and 6). Anteriorly, the basisphenoid rostrum is moderately elongate and dorsoventrally tall, articulating with the laterosphenoid dorsally and pterygoids ventrally. The anterior margin of the basisphenoid rostrum is concave in lateral view and does not project anteriorly past its articulation with the basisphenoid. Along the laterosphenoid-basisphenoid suture, two foramina pierce the basisphenoid (Figure 5). Approximately in line with the trigeminal foramen is an elongate oval opening interpreted as the foramen for the oculomotor nerve (CN III). A second smaller and more circular opening is located just medial to the anterior tip of the orbital process of the quadrate. This opening is interpreted as the foramen for the abducens nerve (CN VI).

Posteriorly, the basisphenoid articulates with the basioccipital, posterolaterally with the quadrates and otoccipitals, and posteroventrally with the pterygoids. The basisphenoid is not visible in occipital view. In ventral view, the basisphenoid exposure is broadly triangular, with its apex extending anteriorly between the pterygoids and elongate, posterolaterally oriented laminae projecting between the basioccipital, otoccipitals, and quadrates (Figure 6). Along the posterior edge of the basisphenoid lie the openings for the median pharyngeal tube (=median Eustachian tube; Colbert, 1946), and lateral Eustachian tube (=pharyngotympanic tube; Dufeau & Witmer, 2015), with the basisphenoid forming the anterior margin of each. Immediately anterior to the median pharyngeal foramen, a single pronounced crest with a flat ventral surface extends the anteroposterior length of the ventral exposure of the basisphenoid. This crest divides two fossae on the basisphenoid, each extending posterolaterally towards the lateral Eustachian foramen. A midline crest on the ventral surface of the basisphenoid common among teleosauroids and basal metriorhynchoids (e.g., *Pelagosaurus* [NMHUK PV OR 32599], the Chinese teleosauroid [IVPP V 1098]; *Machimosaurus buffetauti* [SMNS 91415]; *Charitomenosuchus leedsi* [NHMUK PV R 3320]; *Neosteneosaurus edwardsi* [NHMUK PV R 2865]; and *Opisuchus meieri* [Aiglstorfer et al., 2020]), but in many of these taxa the crest is narrower. The broad flattened crest of MCZ VPRA-1063 most closely resembles that of *Plagiophthalmosuchus*

cf. *gracilirostris* (NHMUK PV OR 33095; Brusatte et al., 2016). It should be noted that this single crest differs from the double crest divided by a shallow sulcus described in a different specimen of *Macrospondylus bollensis* (SNSB-BSPG 1984 I258; Herrera et al., 2018). However, the main difference seems to be that the raised area immediately anterior to the median pharyngeal foramen is concave in SNSB-BSPG 1984 I258 (making the edges into separate crests), but flat in MCZ VPRA-1063 (yielding a single broad crest). The width of the crest may also vary somewhat ontogenetically, as it appears broader in smaller specimens (e.g., GPIT Re 1193/10).

The lateral Eustachian foramina are ovate and positioned slightly dorsal to the median pharyngeal foramen. They are bordered anteriorly by the basisphenoid. The median pharyngeal sinus system is common among crocodylomorphs (Leardi et al., 2020; Nesbitt, 2011; Pol et al., 2013) and is present in all known thalattosuchians (Herrera et al., 2018). Lateral Eustachian tubes with foramina are present in teleosauroids (e.g., *Teleosaurus cadomensis* [see Jouve, 2009]; "*Steneosaurus*" *pictaviensis* [see Herrera et al., 2018]) and basal metriorhynchoids (e.g., *Pelagosaurus* [see Pierce et al., 2017]). However, the lateral Eustachian foramina appear to be lost among metriorhynchids (Herrera et al., 2018).

Basioccipital: The basioccipital is well preserved. It constitutes the majority of the occipital condyle which is slightly taller than wide (Figures 4, 5, 6, and 8). It forms most of the ventral margin of the foramen magnum. Ventral to the occipital condyle lie two large basal tubera. The basal tubera are larger than those of *Indosinosuchus* (PRC-8; Martin et al., 2019) and *Machimosaurus buffetauti* (SMNS 91415), but similar to those of *Proexochokefalos heberti* (MNHN.F 1890-13) and "*?Steneosaurus*" sp. (SMNS 59558). The tubera are slightly wider than tall in occipital view with raised, rugose lateral and ventral margins (presumably attachment sites for the *m. longus* capitis posterior and *m. rectus* capitis anticus major, respectively; Schwarz-Wings, 2014). Each bears a smooth shallow fossa ventrolateral to the occipital condyle. The basioccipital tubera are separated from one another by a deep midline sulcus extending ventrally from the ventral margin of the occipital condyle to the posterior margin of the median pharyngeal foramen (Figure 6). The basioccipital articulates dorsolaterally and laterally with the otoccipitals. The otoccipitals slightly overlap the dorsal portion of the tubera, but otherwise do not contribute to their formation.

On the ventral surface of the skull the basioccipital articulates anteriorly with the basisphenoid in a broad, gently curved suture. At the midpoint of this suture lies the median pharyngeal foramen, of which the basioccipital forms the posterior margin. At the lateral edge of the basisphenoid-basioccipital suture, the basioccipital contributes slightly to the medial part of the posterior margin of the lateral Eustachian foramen (Figure 6).

Ectopterygoid: Both ectopterygoids are preserved, but only their dorsal surface is visible (Figure 1). The ectopterygoid is small and roughly rectangular, though broader at each end than in the middle. It is inclined slightly posteroventrally, articulating with the palatal process of the maxilla anteriorly and medially, the jugal anteriorly and laterally, and the lateral wing of the pterygoid posteriorly. At its articulation with the pterygoid, it sends a short V-shaped process posteriorly along the dorsal surface of the pterygoid, just medial to the short thickened lateral edge of the pterygoid wing. The ectopterygoid forms the posterior half of the lateral margin of the suborbital fenestra.

Pterygoid: The pterygoids are well preserved, but, given the preparation of the specimen, most of their ventral surface remains embedded in matrix (Figures 1–7). The pterygoids are anteroposteriorly elongate, with short wings projecting laterally just anterior to the anteroposterior midpoint. The anterior process of the pterygoid has a broad articulation with the palatine anteriorly and laterally and forms the lateral wall and roof of the nasopharyngeal duct. The articulation with the palatine is complex and Z-shaped in dorsolateral view, with a long, straight suture just dorsal to the suborbital fenestra, leading to an invagination accepting a posterior projection of the palatine, followed by an anteromedially directed suture disappearing into matrix along the ventromedial border of the postnasal fenestra (Figure 7). Additionally, the anterior process of the pterygoid has a narrow articulation with the descending process of the prefrontal (prefrontal pillar), but does not project dorsally to meet the prefrontal and thus does not actually contribute to the pillar itself (Figure 3). The morphology of the anterior process is quite similar to that reported by Jouve (2009) for *Teleosaurus cadomensis*, though he interpreted the fragment of bone articulating with the prefrontal pillar as part of the palatine, instead of the pterygoid. Participation of the pterygoid in the margin of the postnasal fenestra of MCZ VPRA-1063 differs from the condition in *Cricosaurus araucanensis* (Fernández & Herrera, 2009) and potentially *Teleosaurus* (depending on whether the fragment of bone on the inferior end of the prefrontal pillar is part of the palatine or pterygoid).

The lateral wing of the pterygoid is expanded laterally, but narrow anteroposteriorly, especially when compared with the broad, anteroposteriorly elongate pterygoid wings of most neosuchians. It ends laterally at a short, thickened, vertically oriented flat surface, sloping from anterosuperior to posteroinferior. The lateral wing

ends laterally quite a distance from the medial surface of the mandible, and thus the pterygoids probably played a lesser role in buttressing the mandible than in extant crocodylians and likely most mesoeucrocodylians (Busbey, 1995; Holliday & Nesbitt, 2013). The lateral wing articulates with the ectopterygoid anterolaterally, and forms the posterior border of the suborbital fenestra.

Posterior to the lateral wing, the lateral margin of the pterygoid is strongly concave in dorsal view. Posteromedially, the dorsal surface of the pterygoid articulates with the basisphenoid and has a short articulation with the quadrate. In ventral view, the ventral exposure of the basisphenoid projects anteriorly between the pterygoids in a V-shaped suture (Figure 6). This shallow, V-shaped posterior articulation with the basisphenoid is shared with the Chinese teleosauroid (IVPP V 10098), but differs from the broad, U-shaped suture of *Teleosaurus cadomensis* (see Jouve, 2009) or *Pelagosaurus* (NHMUK PV OR 32599). It differs greatly from the elongate, V-shaped articulations of some other teleosauroids such as *Neosteneosaurus edwardsi* (NHMUK PV R 2865).

Palatine: Only part of the dorsal surface of each palatine is visible (Figures 1 and 7). Laterally, it articulates with the medial margin of the palatal process of the maxilla. Posteriorly and medially, it articulates with the anterior process of the pterygoid. The palatine forms the medial margin of the suborbital fenestra and the ventromedial border of the postnasal fenestra. The most anteriorly exposed portion contributes to the lateral wall of the nasopharyngeal duct.

3.3 | Bones of the mandible

Dentary: The posterior portions of both dentaries are preserved, including approximately 12 alveoli (Figure 2). The lateral and ventral surfaces are ornamented with faint, anteroposteriorly aligned grooves, similar to the maxilla. Medially, the dentary articulates with the splenial. Along the preserved portion of the symphysis, of which approximately the posterior one-third is preserved, the dentaries are separated from one another by the splenials. Posteriorly, the dentary contributes to the anterior and part of the dorsal margin of the external mandibular fenestra. Posterodorsally, the dentary contacts what appears to be an elongate, slender coronoid. Posteriorly, the dentary articulates with the surangular in a posteroventrally inclined suture which intersects the dorsal margin of the external mandibular fenestra. Posteroventrally, it articulates with the angular.

Splenial: The splenials are mostly preserved but only their ventral surface is exposed. They contribute extensively to the symphysis as in all thalattosuchians. Along the symphysis, the ventral surface is ornamented similar to the dentary. Anteriorly and laterally, the splenials articulate with the dentaries. Posteriorly, the splenial diverges laterally along the mandibular ramus, and articulates laterally with the angular. In ventral view, the splenial terminates posteriorly approximately in line with the anterior border of the infratemporal fenestra.

Coronoid: In lateral view, an elongate slender bone is present near the dorsal margin of the mandible, articulating along its lateral margin with the dentary and surangular (Figure 2). This is consistent with the morphology and position of the coronoid in other teleosauroids in which this element is highly elongate (relative to its morphology in most other crocodyliform groups), abuts the posterior part of the dentary toothrow, and extends well into the symphysis (e.g., *Charitomenosuchus leedsi* [NHMUK PV R 3320]; *Lemmysuchus* [see Johnson et al., 2017]). A slender elongate anterior process of the coronoid is also present in metriorhynchids (Andrews, 1913) and in at least some sphenosuchians (e.g., *Sphenosuchus acutus* [see Walker, 1990]).

Surangular: The surangular is an anteroposteriorly elongate bone in lateral view (Figure 2). It makes up much of dorsolateral surface of the mandibular ramus. Its surface is relatively unornamented (though the surface is not well preserved anteriorly), with slight anteroposteriorly aligned grooves present in the region of the retroarticular process. Anteriorly it articulates with the dentary, anteromedially with the coronoid, ventrally with the angular, and posteromedially with the articular. The surangular forms the posterior and most of the dorsal borders of the external mandibular fenestra. Interestingly, it appears to possess a very thin anterior process along the ventral margin of the fenestra, excluding the angular from the posterior half of the ventral margin of the external mandibular fenestra. Its suture with the angular is gently sigmoid, with the anterior one-third posterodorsally inclined, the middle one-third approximately horizontal, and the posterior one-third posterodorsally inclined again along the retroarticular process. The posterior process of the surangular strongly narrows posteriorly, extending to the distal end of the retroarticular process. Anteriorly it terminates just posterior to the anterior margin of the orbit. The surangular does not contribute to the glenoid fossa.

Angular: The angular is an elongate bone forming much of the ventral and ventrolateral surface of the mandibular ramus (Figures 2 and 8). Its surface is ornamented with faint grooves, like those of the dentary and maxilla. It articulates with the dentary anteriorly, the splenial anteromedially, the surangular dorsally and the articular and prearticular posteromedially. In ventral view, the long anterior process extends between the

dentary and splenial, terminating just posterior to the posterior margin of the symphysis. It forms the anterior half of the ventral margin of the external mandibular fenestra. Posterior to this fenestra, the angular makes up approximately half of the height of the mandible in lateral view. It extends posteriorly to the distal tip of the retroarticular process. A pronounced groove is present on the retroarticular process just ventral to, and running parallel with, the angular-surangular suture (Figure 2). There is no distinct unornamented region to indicate an insertion of the *M. pterygoideus posterior* onto the lateral surface of the angular, consistent with other thalattosuchians. Posteriorly, the ventral portion of the angular curves medially, forming a lip into which the prearticular (anteriorly) and the articular sit (Figure 8). This ventral shelf of the angular also extends to the distal tip of the retroarticular process.

Articular: The left articular is complete but much of the right one is reconstructed (Figures 2, 4, and 8). The articular is triangular in dorsal view, extending posteriorly in an elongate retroarticular process. As the articulars are preserved in articulation with the quadrates, the morphology of the glenoid fossa cannot be described. A long crest extends posteriorly from the glenoid to the distal tip of the retroarticular process. This crest divides the relatively broad dorsal surface of the articular into two fossae, presumably for attachment of enlarged jaw opening musculature (*M. depressor mandibulae*).

The articular contacts the surangular laterally, the angular ventrolaterally, and the prearticular ventrally (Figure 8). The matrix has not been completely prepared away from its medial surface, so the shape of the suture with the prearticular is unclear. However, its medial surface is a concave surface, oriented ventromedially. As with all thalattosuchians, the articular is not pneumatized and thus lacks a foramen aereum.

Prearticular: Like other thalattosuchians, MCZ VPRA-1063 retains a separate prearticular (Figure 8). It is an elongate, low, triangular element, articulating with the articular dorsally and the angular ventrally and laterally. The posterior process extends beneath the articular approximately half the length of the retroarticular process. The anterior process is elongate, but the area is not prepared anteriorly, so it is unclear whether it contacted a posterior process of the splenial as in *Indosinosuchus* (Martin et al., 2019).

3.4 | Endocranial anatomy

Nasal Cavity: The nasal cavity of MCZ VPRA-1063 is reconstructed for the majority of the preserved skull and rostrum (Figures 9 and 10). The anterior-most region of the cavity and, to a lesser extent, the associated neurovascular canals/extensions of the paranasal sinuses are crushed and not included in the 3D model. The nasal cavity extends posteriorly to the internal (secondary) choana ventral to the cerebrum and pituitary fossa. The morphology of these structures generally resembles the elongate and simplified anatomy of other longirostrine crocodylomorphs, such as *Pelagosaurus typus* and *Gavialis gangeticus* (see Pierce

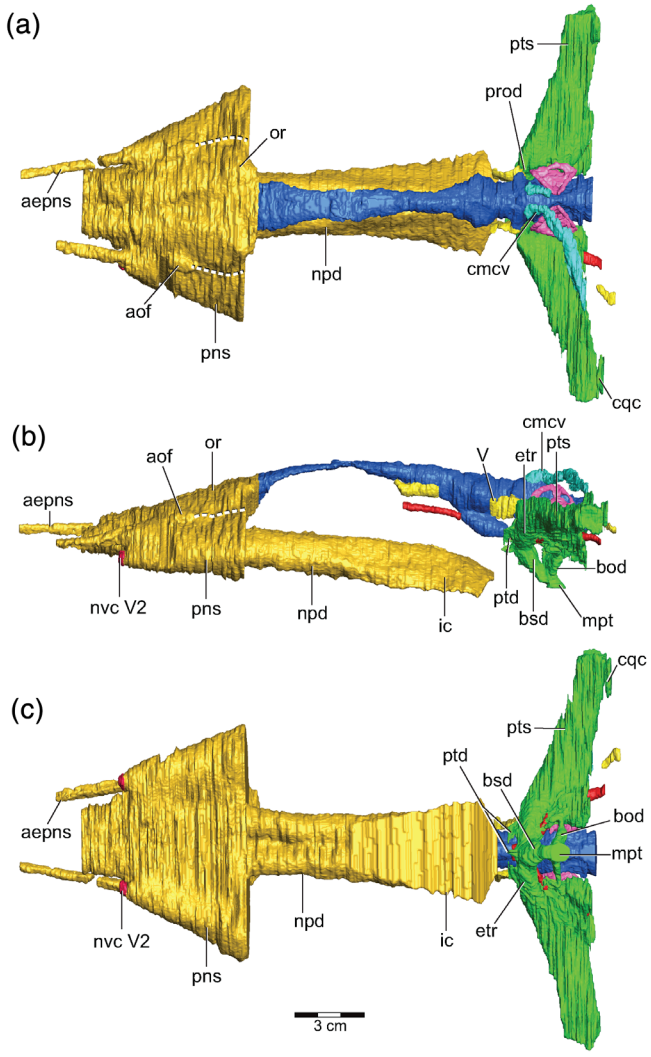

FIGURE 9 Reconstruction of the endocranial anatomy of *Macrospondylus bollensis* (MCZ VPRA-1063) in (a) dorsal view; (b) left lateral view; and (c) ventral view. Dashed lines in (a) and (b) indicate inferred boundary between olfactory region and paranasal sinus. aepns, anterior extension of paranasal sinus; aof, antorbital fenestra; bod, basioccipital diverticulum; bsd, basisphenoid diverticulum; cqc, cranioquadrate canal; etr, recessus epitubaricum; cmcv, caudal middle cerebral vein; ic, internal choana; mpt, median pharyngeal tube; npd, nasopharyngeal duct; nvc V2, maxillary nerve neurovascular canal; or, olfactory region; pns, paranasal (antorbital) sinus; prod, prootic diverticulum; ptd, pterygoid diverticulum; pts, paratympanic sinus. Image credit: Museum of Comparative Zoology, Harvard University

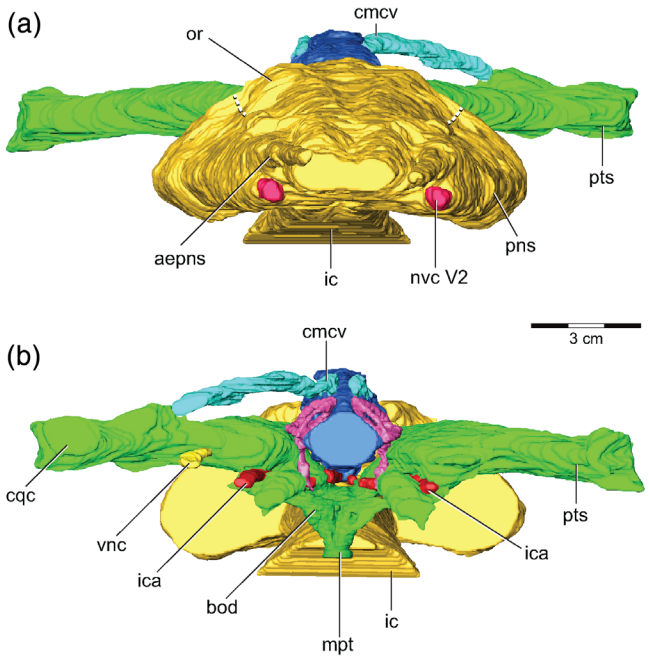

FIGURE 10 Reconstruction of the endocranial anatomy of *Macrospondylus bollensis* (MCZ VPRA-1063) in (a) anterior view and (b) posterior view. Dashed lines in (a) indicate inferred boundary between olfactory region and paranasal sinus. aepns, anterior extension of paranasal sinus; bod, basioccipital diverticulum; cmcv, caudal middle cerebral vein; cqc, cranioquadrate canal; ic, internal choana; ica, internal carotid artery; mpt, median pharyngeal tube; nvc V2, maxillary nerve neurovascular canal; or, olfactory region; pns, paranasal (antoribital) sinus; pts, paratympanic sinus; vnc, vagus nerve canal. Image credit: Museum of Comparative Zoology, Harvard University

et al., 2017) as well as *Cricosaurus araucanensis* (see Herrera, Fernández, & Gasparini, 2013b). The contents of the preserved bony nasal cavity of MCZ VPRA-1063 can be divided into three main components: the olfactory region, the paranasal sinuses and associated neurovascular canals, and the nasopharyngeal duct and internal choana. Following Pierce et al. (2017) we will use the term "olfactory region" to refer to the space containing both olfactory epithelium and potential glandular tissue due to the difficulty of differentiating these soft tissue structures in CT scans of fossil specimens.

The olfactory region of the nasal cavity is immediately anterior to the olfactory bulbs of the cranial endocast. As will be discussed later, there is a subtle, dorsal groove towards the anterior end of the cranial endocast, posterior to the prefrontal pillars, that likely represents the expansion of the olfactory bulbs. Anterior to the bulbs and between the prefrontal pillars are larger and more dorsally bulbous expansions that form the olfactory region of the nasal cavity. The contents of the olfactory region are clearly delimited in the natural endocasts of other crocodylomorph taxa, such as *Cricosaurus araucanensis* (see Herrera, Fernández, & Gasparini, 2013b), *Rhabdognathus* (see Erb & Turner, 2021), and various notosuchian specimens (Fonseca et al., 2020). In metriorhynchids, such as *Cricosaurus araucanensis* (see Herrera, Fernández, & Gasparini, 2013b), the detailed natural endocasts exhibit what appears to be glandular tissue lateral to the olfactory epithelium. However, in less detailed CT scans, this distinction cannot be made. Thus, we infer that the bulbous olfactory region of MCZ VPRA-1063 contained both olfactory epithelium (medially) and glandular tissue (laterally). The olfactory region of MCZ VPRA-1063 is bounded laterally by ventromedially/dorsolaterally directed grooves nearly in line with the long axis of the antorbital fenestra (Figures 9 and 10). The grooves separate the olfactory region from the paranasal sinuses. A mediolaterally wide dorsal midline groove separates the two swellings of the olfactory region, and it is most prominent near the posterior end of the antorbital fenestra. In general, the olfactory region of MCZ VPRA-1063 has morphology intermediate between *Pelagosaurus* and extant taxa, such as *Gavialis gangeticus*. The midline groove is larger than that seen in *Gavialis*, but less conspicuous and extensive compared to *Pelagosaurus typus* (see Pierce et al., 2017). Likewise, the mediolateral width and overall volume of the olfactory region is large compared to extant taxa but noticeably reduced compared to *Pelagosaurus typus* (see Pierce et al., 2017) and *Cricosaurus araucanensis* (see Herrera, Fernández, & Gasparini, 2013b). The glandular tissue of other thalattosuchian specimens has been hypothesized to represent salt glands (Fernández & Gasparini, 2000, 2008; Herrera, 2015; Herrera, Fernández, & Gasparini, 2013b). Pierce et al. (2017) suggest an expanded and bulbous olfactory region may be used as an osteological correlate for the presence of salt glands. The presence of small bulbous expansions of the olfactory region in MCZ VPRA-1063 suggests it may have possessed nasal salt glands that would have been less developed than those of *Pelagosaurus* and much smaller than those of fully pelagic taxa, like *Cricosaurus araucanensis* (see Herrera, Fernández, & Gasparini, 2013b).

Ventrolateral to the olfactory region of the nasal cavity are semi-conical outpouchings that likely represent portions of the paranasal sinus system, and more specifically, the antorbital sinus identified in other thalattosuchians (Fernández & Herrera, 2009; Herrera, Fernández, & Gasparini, 2013b; Pierce et al., 2017). Dorsally, the antorbital sinus is separated from the olfactory region by a groove nearly in line with the opening of the antorbital fenestra, as previously described (Figures 9 and 10). Ventrally, the morphology of the sinus, as well as most boundaries and structures in the ventral midline, are unidentifiable because of poor gray-scale contrast. In

Pelagosaurus typus (see Pierce et al., 2017) and *Cricosaurus araucanensis* (see Herrera, Fernández, & Gasparini, 2013b), the antorbital sinus is smaller and forced into a more ventral location by the expanded olfactory region. The antorbital sinus of MCZ VPRA-1063 is more similar in positioning and size to *Gavialis*, despite the smaller olfactory region of *Gavialis*. The "cone" of the antorbital sinus has a circular base posteriorly and tapers to two canals anteriorly. The canals are dorsoventral to one another with little mediolateral deviation. They are of similar diameter, and due to preservation and CT scan resolution, the dorsal canal could be followed significantly further anteriorly than the ventral canal. In *Pelagosaurus typus* (see Pierce et al., 2017), *Gavialis gangeticus*, and *Cricosaurus araucanensis* (see Herrera, Fernández, & Gasparini, 2013b), a single canal extends anteriorly from the antorbital sinus. It is closely associated with the maxillary teeth posteriorly and takes a more dorsolateral position anteriorly. This canal is interpreted as the dorsal alveolar canal, transmitting branches of the maxillary nerve (V_2) and vessels that supply the maxillary teeth (Pierce et al., 2017). In our specimen, we interpret the ventral canal as transmitting the maxillary nerve and associated vasculature (i.e., dorsal alveolar canal). It has a similar ventral positioning to other taxa, and is closely associated with the maxillary teeth. The dorsal canal has not been noted in other thalattosuchians, though Jouve (2009) described a foramen in this location in *Teleosaurus*. For its reconstructed length, the canal maintains a dorsolateral position to the nasal cavity and narrows slightly anteriorly. We interpret this structure as an anterior extension of the paranasal sinus. However, we cannot rule out an accessory neurovascular canal. More detailed CT scans may provide evidence of branching patterns, and sampling additional taxa will determine if this structure is more widespread among teleosauroids.

The last component of the preserved nasal cavity is the continuation of the airway posteriorly as the nasopharyngeal duct and the internal choana. Ventral to the olfactory region, the formation of the nasopharyngeal duct (i.e., primary choana) is obscured in the CT scan, and it could not be reconstructed. Ventral to the prefrontal pillars and extending posteriorly, the nasopharyngeal duct is roughly triangular in cross-section, wider ventrally and narrowing dorsally. It matches the airway anterior to the olfactory region in width and has a significant midline furrow both dorsally and ventrally. The ventral midline furrow ends posteriorly at the internal choana, which is anteroposteriorly long and widens posteriorly. The internal choana ends posteriorly ventral to the pituitary fossa. Compared to *Cricosaurus araucanensis* (see Herrera, Fernández, & Gasparini, 2013b), the nasopharyngeal duct is longer and more posteriorly positioned. Compared to *Gavialis gangeticus* and *Pelagosaurus typus* (see Pierce et al., 2017), the nasopharyngeal duct is comparatively more robust and consistent in its width along its long axis. Like *Pelagosaurus typus*, MCZ VPRA-1063 lacks the distinct expansion of the nasopharyngeal duct anterior to the internal choana like that seen in *Gavialis*.

Cranial Endocast: The entire length of the cranial endocast, from the olfactory bulbs anteriorly to the foramen magnum posteriorly, is preserved (Figures 9–11). Despite segments of relatively poor contrast in the CT scan, most boundaries of the cranial endocast are defined. Of note, the mid portion of the olfactory tract is damaged and dorsoventrally thin, causing uncertainty in the mediolateral width of the tract. Likewise, the connection between the cerebrum and olfactory tract near the origin of the optic nerve lacks contrast between bone and matrix. The endocast is 145 mm long and 24 mm wide at the lateral maximum of the cerebrum. Generally, the endocast resembles other thalattosuchians, possessing an olfactory tract that accounts for about half of the total length of the endocast (77 mm), a hemispherical cerebral expansion, and obtuse cephalic and pontine flexures (168° and 166°, respectively) (Brusatte et al., 2016; Fernández et al., 2011; Herrera et al., 2018; Pierce et al., 2017). It primarily differs from previously described specimens in its relatively enlarged olfactory bulbs and mediolaterally wide olfactory tract.

The olfactory bulbs are the most anterior component of the cranial endocast. In MCZ VPRA-1063, we identify a lateral and ventral expansion of the olfactory tract posterior to the prefrontal pillars as the olfactory bulbs. A subtle dorsal groove delineates the right and left bulb. In the natural endocast of *Cricosaurus araucanensis* (see MLP 76-XI-19-1; Herrera, Fernández, & Gasparini, 2013b), the olfactory bulbs continue anteriorly beyond the prefrontal pillars and contact the bulbous olfactory region of the nasal cavity. This contact could not be identified in the CT scan, but the space between the prefrontal pillars has been included in the endocast model to better approximate the probable anteroposterior length of the bulbs. The bony separation or partial bony separation between the left and right olfactory bulbs and tracts varies among thalattosuchians. *Cricosaurus araucanensis* (see Herrera et al., 2018; Herrera, Fernández, & Gasparini, 2013b) shows no division, whereas *Pelagosaurus typus* (see Pierce et al., 2017) has a complete division between its olfactory bulbs and tracts. Thalattosuchians are generally thought to have small olfactory bulbs due to their primarily aquatic lifestyles and reduced dependence on airborne olfaction (Herrera, Fernández, & Gasparini, 2013b; Pierce et al., 2017). However, MCZ VPRA-1063 possesses bulbs nearly as wide as the cerebrum at their mediolateral maximum and that

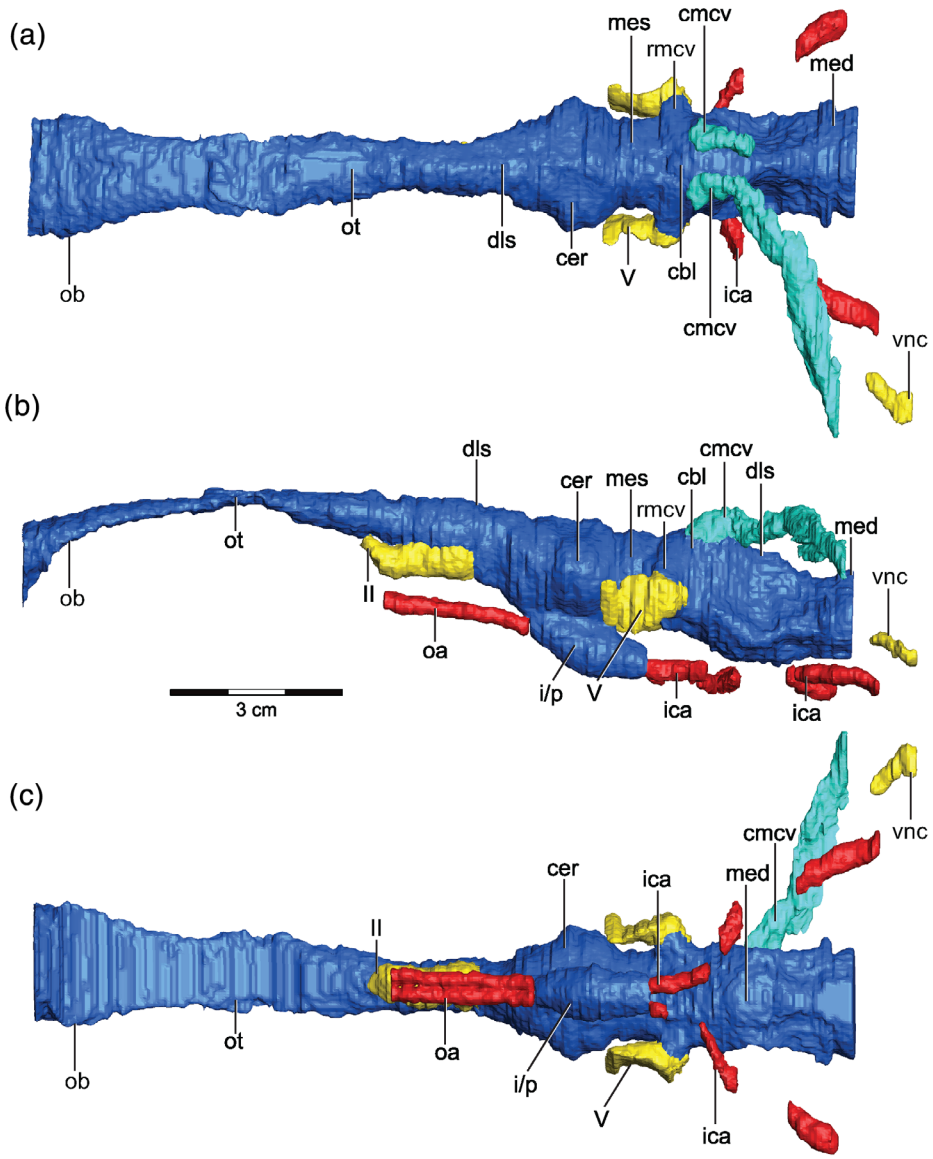

FIGURE 11 Endocast morphology of *Macrospondylus bollensis* (MCZ VPRA-1063) in (a) dorsal view; (b) left lateral view; (c) ventral view. cbl, cerebellum; cer, cerebrum; cmcv, caudal middle cerebral vein; dls, dorsal longitudinal sinus; i/p, infundibulum/pituitary fossa; ica, internal carotid artery; II, optic nerve; med, medulla; mes, mesencephalon; oa, orbital artery; ob, olfactory bulb; ot, olfactory tract; rmcv, rostral middle cerebral vein; V, trigeminal nerve; vnc, vagus nerve canal. Image credit: Museum of Comparative Zoology, Harvard University

differentiate from the olfactory tract more posteriorly than *Cricosaurus araucanensis* (see Herrera et al., 2018; Herrera, Fernández, & Gasparini, 2013b) or *Pelagosaurus typus* (see Pierce et al., 2017).

The olfactory tract connects the olfactory bulbs anteriorly to the cerebrum posteriorly. In MCZ VPRA-1063, the olfactory tract is mediolaterally wide and dorsoventrally thin, but as mentioned previously, these dimensions could be affected by damage to the bone dorsal to the midpoint of the tract. The undivided olfactory tract is gently arched with anterior and posterior ends ventral to the midpoint of the tract. By comparison, the olfactory tract of *Cricosaurus araucanensis* (see Herrera et al., 2018) is mediolaterally thin and has little to no arch along its length. The structure in *Pelagosaurus typus* (see Pierce et al., 2017) is angled anteroventrally and completely divided along the midline.

Anterior to the cerebral expansions and ventral to the olfactory tract, we identify the optic nerve (CN II) protruding from the cerebrum. This area of the CT scan has poor bone-to-matrix contrast, so it is possible the optic nerve initially branches more posteriorly and has a greater degree of separation from the cranial endocast. The region of the endocast around the optic nerve is most similar to *Plagiophthalmosuchus* cf. *gracilirostris* (NHMUK PV OR 33095; Brusatte et al., 2016). Both are mediolaterally narrow, nearly as dorsoventrally deep as the endocast at the cerebral expansions, and anteroposteriorly extended between the cerebral expansions and the optic nerves. In its entirety, the cerebrum is dorsal to the pituitary fossa and extends from the optic nerves anteriorly to the optic lobe posteriorly. As in other thalattosuchians, such as *Cricosaurus araucanensis* (see Herrera et al., 2018), *Pelagosaurus typus* (see Pierce et al., 2017),

Macrospondylus bollensis (see Herrera et al., 2018), and *Plagiophthalmosuchus* cf. *gracilirostris* (see Brusatte et al., 2016), the lateral expansions of the cerebrum in MCZ VPRA-1063 are nearly hemispherical. Modern crocodylians, such as *Gavialis gangeticus* (see Pierce et al., 2017) and *Alligator mississippiensis* (see Witmer & Ridgely, 2008) have cerebra with anterodorsally/posteroventrally angled expansions. The shape and volume of the cerebrum of MCZ VPRA-1063 is most similar to another specimen of *Macrospondylus bollensis* (see Herrera et al., 2018) and *Plagiophthalmosuchus* cf. *gracilirostris* (see Brusatte et al., 2016), which have smaller and less laterally expanded cerebra compared to *Cricosaurus araucanensis* (see Herrera et al., 2018) and *Pelagosaurus typus* (see Pierce et al., 2017). They also lack the dorsal groove between the cerebral hemispheres seen in *Pelagosaurus typus* (see Pierce et al., 2017).

In MCZ VPRA-1063, the infundibulum and pituitary protrude from the ventral aspect of the cerebrum and extend posteriorly. The pituitary is long, and its posterior half runs parallel to the long axis of the endocast. The infundibulum is elongated and anterodorsally/posteroventrally angled at its connection to the anterior edge of the diencephalon. As in other thalattosuchians, the pituitary fossa is enlarged and more parallel to the endocast compared to modern crocodylians (Brusatte et al., 2016; Pierce et al., 2017). The fossa of MCZ VPRA-1063 most closely resembles another specimen of *Macrospondylus bollensis* (see Herrera et al., 2018), as both are more anteroposteriorly elongate and less bulbous than in *Cricosaurus araucanensis* (see Herrera et al., 2018) and *Pelagosaurus typus* (see Pierce et al., 2017).

In MCZ VPRA-1063, a tubular region, with slight mediolateral expansions, posterior to the cerebrum and anterior to the trigeminal nerves represents the optic lobe (Figure 11). The endocasts of modern crocodylians frequently lack noticeable expansions for the optic lobe (see *Gavialis gangeticus* [Pierce et al., 2017] and *Crocodylus johnstoni* [Witmer, Ridgely, Dufeau, & Semones, 2008]). However, there is likely an ontogenetic component as young *Alligator mississippiensis* more clearly possess the feature (see Dufeau & Witmer, 2015). At the location of the optic lobe, the endocasts of most thalattosuchians have a smooth, concave transition from the posterior cerebrum to the mediolaterally wide rostral middle cerebral vein and trigeminal nerve (e.g., *Plagiophthalmosuchus* cf. *gracilirostris* [Brusatte et al., 2016]). *Pelagosaurus typus* (see Pierce et al., 2017), in contrast, exhibits an anteroposteriorly elongate and mostly tubular optic lobe that closely resembles MCZ VPRA-1063. The specimen of *Macrospondylus bollensis* described by Herrera et al. (2018) has a concave optic lobe region, similar to *Plagiophthalmosuchus* (Brusatte et al., 2016). Although both are assigned to *Macrospondylus bollensis*, the specimen in Herrera et al. (2018) is smaller than the specimen presented here, and this might explain some of the morphological differences.

The cerebellum is large as in the thalattosuchians *Pelagosaurus typus* (see Pierce et al., 2017), *Plagiophthalmosuchus* cf. *gracilirostris* (see Brusatte et al., 2016), and another specimen of *Macrospondylus bollensis* (see Herrera et al., 2018), as well as in the dyrosaurid *Rhabdognathus* (Erb & Turner, 2021). Similar to these taxa, and unlike the cerebellum of *Gavialis* (see Pierce et al., 2017), the cerebellum of MCZ VPRA-1063 projects dorsally above the dorsal plane of the endocast formed by the cerebrum and optic lobes. The medulla closely resembles that of another *Macrospondylus bollensis* (see Herrera et al., 2018), though the medulla of MCZ VPRA-1063 has a more pronounced curvature to the ventral margin. The vestibular depression is expressed low, near the ventral margin of the medulla. This is similar to other thalattosuchians but unlike the dyrosaurid *Rhabdognathus* (Erb & Turner, 2021). There is no ventral swelling posterior to the vestibular depression like that described for *Pelagosaurus typus*, which was interpreted to be part of the basal artery (Pierce et al., 2017). The portion of the medulla in MCZ VPRA-1063 posterior to the vestibular depression is similar to that of *Plagiophthalmosuchus* cf. *gracilirostris* (see Brusatte et al., 2016), and unlike the foreshortened medulla described by Pierce et al. (2017) for *Pelagosaurus typus*.

Cranial Nerves and Vasculature: Despite identifying most of their foramina on the external surface of the skull, few cranial nerves are visible on the endocast. As mentioned previously, the optic nerve (CN II) protrudes anteriorly from the cerebrum ventral to the olfactory tract (Figure 11). This differentiation occurs mostly anterior to, and in line with, the lateral maximum of the cerebral expansion, while in *Cricosaurus araucanensis* (see Herrera et al., 2018) and *Pelagosaurus typus* (see Pierce et al., 2017), the optic nerve branches more ventral to the expansions. In other thalattosuchian and modern crocodylian endocasts, the optic nerve is anteroposteriorly short to nonexistent because it is minimally bounded by bone. However, in MCZ VPRA-1063, we could reconstruct it for a significant distance, making it similar to but proportionally shorter than the structure in *Rhabdognathus* (see Erb & Turner, 2021). Posterior to the cerebrum and optic lobe, the path of the trigeminal nerve root (CN V) through the trigeminal foramen and the expansion of the trigeminal fossa are identified (Figure 11). The trigeminal fossa is an elongate, rounded cavity bounded by the laterosphenoid, prootic, and orbital process of the quadrate. In the trigeminal fossa of MCZ VPRA-1063, a projection of the prootic divides two

openings; an anteromedial and a posterolateral foramen. The anteromedial foramen is the trigeminal foramen, while the posterolateral foramen appears associated with the pneumatic spaces surrounding the middle ear and invading the quadrate. The bone of the prootic projection was difficult to discern in the CT scan. However, the anterior region of the trigeminal fossa contained the trigeminal ganglion connecting to the cranial endocast through the trigeminal foramen (Figure 9). The posterolateral portion of the fossa likely contained a different structure, confluent with the paratympanic sinus posterolaterally (Figure 9). A connection between the trigeminal fossa and paratympanic sinuses is seen in other thalattosuchians, such as "*Metriorhyhchus*" cf. *westermanni* (Fernández et al., 2011). Lastly, the vagus canal (carrying cranial nerves IX–XI) was identified on the left side of the CT scan (Figures 10 and 11). However, it could only be followed anteriorly a short distance, and it lacked the resolution to determine if the canal divides anteriorly.

The rostral and caudal middle cerebral veins, dorsal longitudinal sinus, and internal carotid and orbital arteries were identified for MCZ VPRA-1063 (Figure 11). The rostral middle cerebral vein is represented by a lateral protrusion immediately dorsal to the trigeminal nerve root. This vein exits into the trigeminal fossa and is commonly identifiable in thalattosuchians (Herrera et al., 2018). The caudal middle cerebral vein is a conspicuous, anteroposteriorly extended cavity that projects from the dorsolateral edge of the cranial endocast posterior to the trigeminal fossa and anterior to the dorsal tip of the endosseous labyrinth. Posteriorly, the vein makes a sharp turn and travels posterolaterally through the temporo-orbital canal where it has a communication with the supratemporal fenestra via the temporo-orbital foramen (Figure 11). Laterally, the temporo-orbital canal is confluent with the paratympanic sinus medial to the cranioquadrate canal (Figures 9 and 10), rather than meeting the cranioquadrate canal as in *Cricosaurus araucanensis* (see Herrera et al., 2018) or "*Metriorhynchus*" cf. *westermanni* (see Fernández et al., 2011). The path of the right caudal middle cerebral vein could not be traced laterally. The general features and directionality of the caudal middle cerebral vein is consistent among thalattosuchians. The vein of MCZ VPRA-1063 does not extend as far dorsally as other teleosauroids, such as *Plagiophthalmosuchus* cf. *gracilirostris* (see Brusatte et al., 2016) and a different specimen of *Macrospondylus bollensis* (see Herrera et al., 2018), but rather travels closer to the paratympanic sinus like *Pelagosaurus typus* (see Pierce et al., 2017). The dorsal longitudinal sinus is a rounded midline ridge on the dorsal surface of the cranial endocast. In MCZ VPRA-1063, it extends from near the branching point of the optic nerve to the caudal middle cerebral veins and appears to expand or split dorsal to the trigeminal nerves similar to "*Steneosaurus*" *pictaviensis* (see Wharton, 2000). The ridge is less pronounced than in *Cricosaurus araucanensis* (see Herrera et al., 2018) but similar in size and length to *Plagiophthalmosuchus* cf. *gracilirostris* (see Brusatte et al., 2016).

Entering the skull through large, ventrolaterally directed foramina in the otoccipital (Figures 4 and 6), the internal carotid arteries pass through the internal carotid canals to reach the posterior pituitary fossa (Figures 9–11). The canals could not be traced to the foramina due to poor contrast of the CT scan, but the remainder of their length was reconstructed. Anterior to the foramina, the canals arch dorsomedially for a short distance and then maintain a consistent dorsoventral height. In ventral view, they reach the pituitary fossa following a roughly sigmoidal configuration. The internal carotid canals are not fully ossified, with two portions that could not be segmented where they pass through the paratympanic sinus. The left canal is larger or more conspicuously preserved than the right, especially just posterior to the pituitary fossa. Other teleosauroids, like *Macrospondylus bollensis* (see Herrera et al., 2018) and *Plagiophthalmosuchus* cf. *gracilirostris* (see Brusatte et al., 2016), have more dorsoventral variability in height along the path of the carotid canals. Anterior to the pituitary fossa, lie prominent canals transmitting the orbital arteries (and veins) as in other thalattosuchians, such as *Cricosaurus araucanensis* (see Herrera et al., 2018) and *Plagiophthalmosuchus* cf. *gracilirostris* (see Brusatte et al., 2016), as well as in the dyrosaurids *Rhabdognathus* (Erb & Turner, 2021) and *Hyposaurus* (NJSM 23368; pers. obs.). In MCZ VPRA-1063, the orbital artery canals are slightly smaller in diameter than the internal carotid canals and continue in close association until the anterior edge of the laterosphenoid.

Endosseous labyrinth: The complete right and left endosseous labyrinths are reconstructed for MCZ VPRA-1063. This includes the semicircular canals and vestibule of the vestibular apparatus dorsally and the cochlear duct ventrally (Figure 12). Following the measurement scheme of Pierce et al. (2017), the labyrinth height and width are 25 and 21 mm, respectively, and the cochlear duct height is 14 mm for the right and 16 mm for the left. The general organization of the bony inner ear is consistent among crocodylomorphs (e.g., Brusatte et al., 2016; Dufeau & Witmer, 2015; Kley et al., 2010; Schwab et al., 2020; Witmer et al., 2008), but the proportions and robusticity of the structures reflect ecological and behavioral differences (Schwab et al., 2020). The anterior and posterior semicircular canals of MCZ VPRA-1063 are "pyramidal", having sharp dorsal and ventral curves with little curvature along the rest of their length. This feature

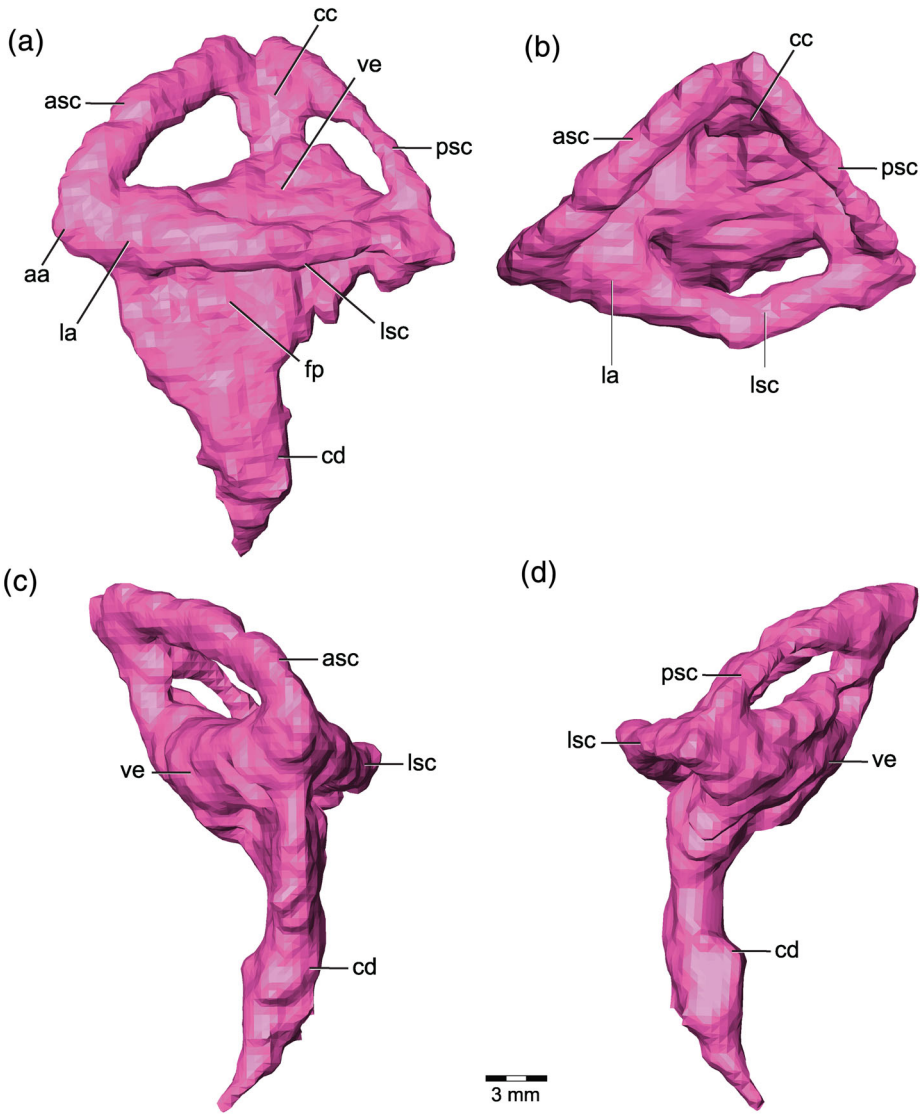

FIGURE 12 Left endosseous labyrinth of *Macrospondylus bollensis* (MCZ VPRA-1063) in (a) left lateral view; (b) dorsal view; (c) anterior view; and (d) posterior view. aa, anterior ampula; asc, anterior semicircular canal; cc, common crus; cd, cochlear duct; fp, fenestra perilymphatica; la, lateral ampulla; lsc, lateral semicircular canal; psc, posterior semicircular canal; ve, vestibule. Image credit: Museum of Comparative Zoology, Harvard University

seems consistent among thalattosuchians, but it also appears in some extant crocodylians, suggesting phylogenetic variability (Brusatte et al., 2016; Pierce et al., 2017). The anterior and posterior semicircular canals of MCZ VPRA-1063 have nearly the same dorsal height with the anterior or posterior rising just slightly above the other depending on which side of the specimen is viewed. Asymmetry could be preservational or caused by the lack of clarity of the CT scan. The anterior semicircular canal is longer than the posterior and is greater in diameter. It creates a larger window between itself and the common crus and vestibule than the posterior canal. The posterior semicircular canal has a slight constriction near its midpoint on both the right and left, though it is more distinct on the left (Figure 11). The common crus has a diameter intermediate to the diameters of the anterior and posterior semicircular canals and appears larger for the left inner ear than the right. The diameter of the lateral semicircular canal is more similar to the anterior canal and it forms a relatively low, straight-edged arch with the lateral pinnacle of the arch at its midpoint. Fully pelagic, derived thalattosuchians, such as *Cricosaurus araucanensis* (see Herrera et al., 2018), evolved compact but robust semicircular canals (Schwab et al., 2020). However, the inner ear morphology of MCZ VPRA-1063 noted above is mostly within the range of variation observed in other near-shore teleosauroids and basal metriorhynchoids (Brusatte et al., 2016; Herrera et al., 2018; Pierce et al., 2017). Of note, the thickness of the anterior semicircular canal relative to the posterior semicircular canal is greater in MCZ VPRA-1063 than in other thalattosuchians.

Ventrally, the triangular cochlear duct, which is related to hearing prowess (e.g., Walsh, Barrett, Milner, Manley, & Witmer, 2009), extends from the vestibular apparatus to a point beyond the ventral border of the cranial endocast (Figure 10). Just ventral to the vestibular apparatus, the cochlear duct shifts anteriorly, creating a convex anterior

edge and a concave posterior edge. It straightens and narrows as it passes the cranial endocast. Along its path, the duct has a slight medial curve, wrapping beneath the medulla. The morphology and relative size of the cochlear duct most closely resemble another *Macrospondylus bollensis* specimen (see Herrera et al., 2018) and *Pelagosaurus typus* (see Pierce et al., 2017). *Cricosaurus araucanensis* (see Herrera et al., 2018) and *Plagiophthalmosuchus* cf. *gracilirostris* (see Brusatte et al., 2016) have smaller cochlear ducts that barely extend past or are in line with the ventral margin of the endocast.

Paratympanic Sinus: An elaborate and interconnected series of pneumatic diverticula lined with pharyngeal-derived epithelium connects the middle ear cavity to the pharynx in crocodyliforms. It is derived from two embryological systems: the median pharyngeal sinus and the larger pharyngotympanic sinus (Dufeau & Witmer, 2015). Compared to extant crocodylians, the paratympanic sinus of thalattosuchians is less complex owing to the absence of several diverticula (Brusatte et al., 2016; Herrera et al., 2018; Pierce et al., 2017). The paratympanic sinus of MCZ VPRA-1063 was reconstructed bilaterally (Figures 9 and 10). However, the contrast and resolution of the CT scan prevented confident delineation of several boundaries, especially those of the lateral and posterior surfaces.

In the ventral midline, between the basioccipital and basisphenoid, the large and circular median pharyngeal foramen (Figure 6) connects the pharynx to the median pharyngeal tube. The median pharyngeal tube extends anterodorsally from the foramen and bifurcates dorsally into anterior and posterior sinuses and canals. The posterior division (posterior communicating canal, sensu Miall, 1878) is primarily formed by the basioccipital diverticula, creating one of the connections between the median pharyngeal sinus and the pharyngotympanic sinus (Dufeau & Witmer, 2015). The left and right basioccipital diverticula and their connections are triangular in anterior and posterior view, being narrow ventrally and expanding dorsally to become mediolaterally wide and flat at their dorsal edge. A midline fold delimits the left and right sides of the sinus, and dorsolaterally the sinus connects to the middle ear cavity near the lateral eustachian foramina. Returning to the division of the median pharyngeal tube, the anterior sinus, formed by the basisphenoid diverticula, continues anterodorsally in the midline, expands dorsally, and bifurcates ventral to the internal carotid arteries. Lateral to the internal carotid arteries, the basisphenoid diverticula meet with the recessus epitubaricum of the pharyngotympanic sinus and continue dorsolaterally to communicate with the middle ear cavity. Anteriorly directed projections extend from the midline basisphenoid diverticula and recessus epitubaricum. These structures might be artifacts of the CT scan, or they could be indicative of the pterygoid diverticulum, ambiguously identified in other thalattosuchians (e.g., *Macrospondylus bollensis* [see Herrera et al., 2018]) and differing in morphology.

The middle ear cavity resembles an elongate rectangle that narrows laterally (Figures 9 and 10). The narrowing is primarily caused by the anterior face of the cavity, which is angled posterolaterally. The posterior, dorsal, and ventral surfaces of the middle ear cavity are primarily flat without major grooves and ridges. However, the lack of features could be an artifact of the CT scan. As in other thalattosuchian specimens (e.g., *Macrospondylus bollensis* [Herrera et al., 2018]; *Pelagosaurus typus* [Pierce et al., 2017]), we do not identify infundibular, quadrate, or intertympanic diverticula. Unlike another specimen of *Macrospondylus bollensis* (see Herrera et al., 2018), we could not reconstruct the distinct shelf of the otoccipital diverticula protruding from the posterior middle ear cavity and partially pneumatizing the otoccipital (though this could be due to the lower resolution of our scan). On the ventral surface of the middle ear cavity, near the connection of the basioccipital diverticula, dorsoventrally short and mediolaterally wide pharyngotympanic tubes connect the middle ear cavity to the lateral Eustachian foramina (Figure 6). In *Pelagosaurus typus* (see Pierce et al., 2017), no pharyngotympanic tubes were identified. The small to nonexistent tubes in thalattosuchians and the significant dorsal displacement of the lateral eustachian foramina compared to the median pharyngeal foramen suggest soft tissue connections to the pharynx in living individuals. Lastly, the anteromedial portion of the middle ear cavity is confluent with the trigeminal fossa. A similar connection has been recognized in other thalattosuchians, such as "*Metriorhyhchus*" cf. *westermanni* (see Fernández et al., 2011), but it is larger in MCZ VPRA-1063. This feature was considered previously in reference to the trigeminal nerve and fossa, and see the discussion for possible soft tissue contents. Positioned between the root of the trigeminal nerve and the semicircular canals, a small, medial outpouching of the paratympanic sinus may represent the prootic diverticulum. The paratympanic sinuses of MCZ VPRA-1063 are broadly similar to the sinuses of other thalattosuchian specimens, such as another *Macrospondylus bollensis* (see Herrera et al., 2018) and *Pelagosaurus typus* (see Pierce et al., 2017). In addition to differences mentioned above, the median pharyngeal tube, basioccipital diverticula, and basisphenoid diverticula are noticeably more vertical than in any observed thalattosuchian. In *Alligator mississippiensis*, these structures become more vertical through ontogeny (Dufeau & Witmer, 2015), so it is possible MCZ VPRA-1063 is a later ontogenetic stage than other described thalattosuchian specimens, which is supported by its larger size.

4 | DISCUSSION

4.1 | Trigeminal fossa morphology among thalattosuchians

The enlarged trigeminal fossa of MCZ VPRA-1063 houses two large openings of approximately equal size, a medially positioned trigeminal foramen and a lateral foramen communicating with the paratympanic sinus posteriorly (which we will term "Foramen 2" for ease of discussion; Figure 5). Why a pneumatic diverticulum would extend into the trigeminal fossa is unclear. It seems more likely to us that this opening transmitted neurovasculature, rather than a part of the pneumatic diverticulum (though we cannot exclude the possibility of a pneumatic structure filling at least part of this opening). However, the identity of neurovasculature traversing Foramen 2 is uncertain. It is probable that this foramen transmitted the tympanic branch of the trigeminal (as interpreted for smaller foramina in "*Metriorhynchus*" cf. *westermanni* [Fernández et al., 2011] and *Pelagosaurus* [Holliday & Witmer, 2009]), but the large size of the opening suggests the presence of other soft tissue structures. In *Pelagosaurus* and other metriorhynchoids, the trigeminal foramen is often bilobate, with the inferior lobe interpreted as the exit for the trigeminal nerve and the superior as the exit for the rostral middle cerebral vein (Fernández et al., 2011; Herrera et al., 2018; Holliday & Witmer, 2009). The trigeminal foramen of MCZ VPRA-1063 is also somewhat bilobate due to the posterior projection of the laterosphenoid along its anterior margin. Thus, we interpret the dorsal portion of the trigeminal foramen of MCZ VPRA-1063 as transmitting the rostral middle cerebral vein. The surface of the prootic strut separating the trigeminal foramen from Foramen 2 is concave, suggesting the rostral middle cerebral vein may have passed posterolaterally across its surface towards Foramen 2. Here we propose it would join the lateral head vein which passes through Foramen 2. From there, continuing through the paratympanic sinus to join the temporo-orbital vein before exiting the cranioquadrate canal as the stapedial vein.

Regardless of what passes through this Foramen 2, the occurrence of a second large foramen within the trigeminal fossa bordered by a thin strut of prootic may be relatively common among teleosauroids. While *Plagiophthalmosuchus* appears to have a single, circular opening in the trigeminal fossa (Brusatte et al., 2016), *Machimosaurus buffetauti* (SMNS 91415) and *Proexochokefalos heberti* (MNHN.F 1890–13) have a morphology very similar to MCZ VPRA-1063 (Figure 13). Herrera et al. (2018) also mention this configuration in another specimen of *Macrospondylus bollensis* (SNSB-BSPG 1890 I5). How widespread this condition may be among teleosauroids is difficult to discern, since the dorsoventral crushing of most specimens typically damages or destroys this region. Among metriorhynchoids, both *Pelagosaurus* and "*Metriorhynchus*" cf. *westermanni* were described as having smaller foramina in this location, connecting the trigeminal fossa and paratympanic sinus (Fernández et al., 2011; Holliday & Witmer, 2009). The CT scan of another specimen of *Pelagosaurus* (BRLSI M1413; Ballell, Moon, Porro, Benton, & Rayfield, 2019) shows a larger connection between the trigeminal fossa and paratympanic space posterolateral to the trigeminal foramen (pers. obs.). This posterolateral opening is similar in height to the trigeminal foramen but is mediolaterally narrower. This opening has been interpreted as transmitting the tympanic branch of the trigeminal nerve (Fernández et al., 2011; Holliday & Witmer, 2009) or part of the lateral head vein (Holliday, 2006). Thus, an exposed second opening in the trigeminal fossa may be synapomorphic for Thalattosuchia, becoming enlarged in some teleosauroids. Among crocodylomorphs, the only other taxon of which

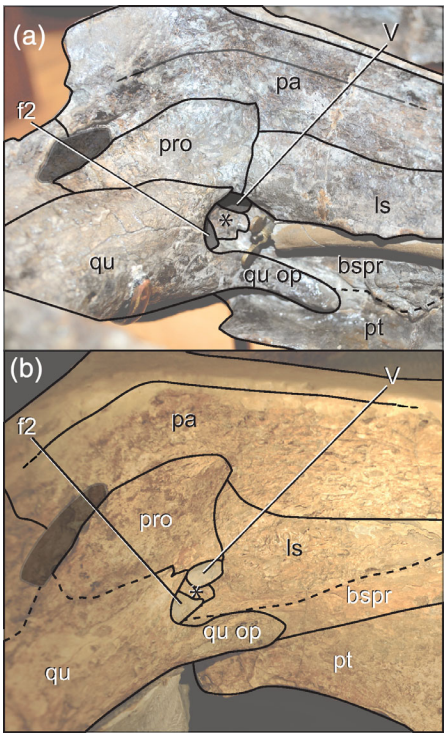

FIGURE 13 Comparison of the trigeminal fossa region of teleosauroids showing a slender process of prootic (*) separating the trigeminal foramen from Foramen 2. Photographs with superimposed line interpretations in oblique dorsolateral view. (a) *Proexochokefalos heberti* (MNHN 1890-13; left side reflected for ease of comparison) and (b) *Machimosaurus buffetauti* (SMNS 91415). bspr, basisphenoid rostrum; f2, "Foramen 2"; ls, laterosphenoid; pa, parietal; pro, prootic; pt, pterygoid; qu, quadrate; qu op, orbital process of quadrate; V, trigeminal foramen

we are aware with a second opening in the trigeminal fossa, similar in size to the trigeminal foramen (and lateral to it) is *Mourasuchus nativus*, a caimanine crocodylian (Bona, Degrange, & Fernández, 2013). This was also interpreted as transmitting the tympanic branch of the trigeminal, and they remarked that the vasculature of the trigeminal fossa may have been hypertrophied.

4.2 | Hypertrophied cephalic vasculature

The cephalic vasculature of thalattosuchians is enlarged relative to most crocodylomorphs. This is evidenced by notable enlargement of the internal carotids, orbital arteries, rostral and caudal middle cerebral veins, temporo-orbital vein, and dorsal venous sinus (Figure 11). Aspects of this have been noted by previous authors (Wharton, 2000; Fernández et al., 2011; Herrera, Fernández, & Gasparini, 2013b; Herrera et al., 2018; Herrera & Vennari, 2015; Brusatte et al., 2016; Pierce et al., 2017). Several functional implications of such enlargement have also been proposed:

1. Osmoregulation (Brusatte et al., 2016; Herrera et al., 2018; Herrera, Fernández, & Gasparini, 2013b; Pierce et al., 2017)
2. Thermoregulation (Herrera et al., 2018)
3. Mitigation of hydrostatic pressure (Herrera et al., 2018)

We will cover each of these functions in turn and note the contributions of the new specimen to each.

Osmoregulation: The most common explanation for the presence of hypertrophied cephalic vasculature, primarily the internal carotids and orbital arteries, is to support the secretory function of salt glands (Brusatte et al., 2016; Herrera et al., 2018; Herrera, Fernández, & Gasparini, 2013b; Pierce et al., 2017). Herrera, Fernández, and Gasparini (2013b) suggested, based on studies of extant birds (e.g., Gerstberger, 1991), that increased size of the internal carotid would increase the rate of blood flow to the nasal salt glands preserved as natural endocasts in *Cricosaurus*. Brusatte et al. (2016) added the observation that the orbital artery (a branch of the internal carotid) is also enlarged in *Plagiophthalmosuchus*, and used this to argue that this increased blood flow to the orbital region implied the presence of salt glands in teleosauroids. MCZ VPRA-1063 supports both of these hypotheses as it confirms the presence of enlarged orbital arteries in another teleosauroid, and the preserved olfactory region shows slight swellings in the expected location of the nasal salt glands. The inferred small size of the salt glands in MCZ VPRA-1063 relative to *Pelagosaurus* (Pierce et al., 2017) and *Cricosaurus* (e.g., Fernández & Gasparini, 2008), is consistent with the hypothesis of Fernández and Gasparini (2008) that teleosauroid salt glands would have reduced secretory capacity relative to metriorhynchids (see additional discussion of salt glands below). However, as noted by Herrera et al. (2018), evidence for salt glands in a teleosauroid is still indirect and the discovery of natural casts (as in *Cricosaurus*) would further solidify this interpretation.

Thermoregulation: Herrera et al. (2018) suggested a potential thermoregulatory function for the enlargement of the cephalic vasculature in thalattosuchians, citing the heavy vascularization of the orbital region in extant crocodylians. Porter, Sedlmayr, and Witmer (2016) suggested that these vascular plexuses in the orbit (among other locations) may allow crocodylians to regulate the temperature of neurosensory tissues. Blood from the orbit may flow through the orbital vein to the cavernous sinus. The venous sinuses of the brains of thalattosuchians are hypertrophied relative to other crocodylomorphs, with notable enlargement of the dorsal longitudinal sinus and enlarged rostral and caudle middle cerebral veins. An enlarged pituitary fossa in thalattosuchians has been noted in prior studies (e.g., Brusatte et al., 2016; Herrera et al., 2018; Pierce et al., 2017). Pierce et al. (2017) suggested this enlargement may result from an enlarged pituitary, with the functional significance that the posterior pituitary has an antidiuretic effect which may have helped thalattosuchians to prevent dehydration. Another potential driver of pituitary fossa enlargement could be an expansion of the cavernous sinus, an idea consistent with overall venous sinus enlargement. These two hypotheses (osmoregulatory function of an enlarged pituitary and thermoregulatory function of an enlarged cavernous sinus) are not mutually exclusive. Endocranial sinuses have anastomotic connections to areas implicated in thermoregulatory heat exchange in extant crocodylians: the orbit via the aforementioned orbital veins, and connections with the temporal region via anastomotic connections with temporo-orbital vein. Holliday, Porter, Vliet, and Witmer (2019) proposed that the temporo-orbital vasculature in the supratemporal fossa may play a role in heating or cooling the brain by acting as a thermal window for heat exchange. In addition to possessing hypertrophied cranial vasculature, thalattosuchians also possess extremely large supratemporal fenestrae. Thus, the potential for heat exchange in this region in thalattosuchians would have exceeded that of extant crocodylians. However, this function of the supratemporal fossa requires further validation in extant crocodylians beyond the pilot study presented in Holliday et al. (2019), as well as more detailed analysis of the supratemporal fossa of thalattosuchians.

Mitigation of hydrostatic pressure: Herrera et al. (2018) also proposed the enlargement of the cephalic vasculature may help to mitigate the effects of hydrostatic

pressure on neural tissues. We are unaware of any effects of hydrostatic pressure on neural tissues that could be alleviated by increased blood flow or volume. However, increased vascularity of the middle ear and other pneumatic spaces in some marine mammals (e.g., pinnipeds; cetaceans) is an adaptation to diving, where the engorgement of venous plexuses in the walls of these spaces helps to accommodate the decrease in air volume during descent (Costidis & Rommel, 2012; Stenfors, Sadé, Hellström, & Anniko, 2001). That thalattosuchians possess reduced cranial pneumatization relative to other crocodylomorphs has been suggested as a possible adaptation to diving (Brusatte et al., 2016), and perhaps the enlarged cranial vasculature also helps to mitigate pressure changes in the cranial pneumatic sinuses. However, this function of venous plexuses is currently only known in marine mammals, so this remains conjecture for Thalattosuchia.

4.3 | Implications of the olfactory and paranasal region for the evolution of marine adaptations in Thalattosuchia

This work includes the first description of the nasal cavity of a teleosauroid. In general, MCZ VPRA-1063 shows simplified, conical paranasal sinuses, consistent with other longirostrine crocodylomorphs (Pierce et al., 2017). However, the paranasal sinus of *Macrospondylus bollensis* appears somewhat more elaborate than that described for metriorhynchoids (*Pelagosaurus* [Pierce et al., 2017]; *Cricosaurus* [Herrera, Fernández, & Gasparini, 2013b]) in that it possesses an elongate, canal-like anterior extension into the maxilla (Figures 9 and 10). A potentially similar anterior extension was proposed in *Teleosaurus* by Jouve (2009) based on a foramen present on the medial surface of the maxilla, so this feature may be widespread among teleosauroids, but this requires data from additional specimens.

The nasal cavity is of particular interest in tracing the evolution of salinity tolerance in Thalattosuchia. In metriorhynchids, this space housed enlarged nasal salt glands (known from numerous natural endocasts; Fernández & Gasparini, 2000, 2008; Herrera, 2015). Enlarged salt glands have also been inferred in this region in the basal metriorhynchoids *Pelagosaurus* (Pierce et al., 2017) and *Zoneait* (Wilberg, 2015a) based on bulbous expansions of the olfactory region. In MCZ VPRA-1063, the portion of the olfactory region posteromedial to the antorbital fenestra is subtly enlarged relative to the comparable area in *Gavialis*, but significantly less inflated than in *Pelagosaurus* (Pierce et al., 2017). This suggests that *Macrospondylus* (and potentially teleosauroids in general), possessed nasal salt glands, but these were less developed and of lower secretory capacity than those of metriorhynchoids (as predicted by Fernández & Gasparini, 2008; Brusatte et al., 2016). Interestingly, the presumed salt glands of *Pelagosaurus*, the basal-most known metriorhynchoid, are already significantly enlarged relative to those of teleosauroids. This suggests that despite being found in the same paleoenvironment, *Pelagosaurus* was better able to osmoregulate than *Macrospondylus*. This may have been a preadaptation in the earliest metriorhynchoid which sparked the invasion of pelagic ecosystems by later members of the group, while teleosauroids predominantly remained in coastal and estuarine environments.

Related to the issue of the nasal salt glands is the identity of the antorbital opening in thalattosuchians. Recent work has interpreted the antorbital opening of *Pelagosaurus* and teleosauroids as a reduced antorbital fenestra, homologous with that of other archosaurs (Leardi et al., 2012). However, in metriorhynchids, the ancestral antorbital fenestra is thought to have closed (internalizing the antorbital sinus), and a neomorphic opening to have formed for drainage of the nasal salt gland ("preorbital opening" sensu Fernández & Herrera, 2009; Leardi et al., 2012). If teleosauroids (and *Pelagosaurus*) possess nasal salt glands, then presumably these glands require an external drainage, and the nearby antorbital opening is a likely candidate (Pierce et al., 2017). This suggests that the very different morphology of the antorbital fenestra/preorbital opening of metriorhynchids may in fact be a modification of the antorbital fenestra of other thalattosuchians, potentially in response to the enlargement and increased secretory capacity of the salt glands. If so, this opening in metriorhynchids may be homologous with the archosaurian antorbital fenestra. Alternatively, it is possible that the antorbital fenestra was closed earlier in evolutionary history, and that a neomorphic opening for salt gland drainage appeared in the common ancestor of Thalattosuchia, being later elaborated by metriorhynchids. However, complicating this interpretation is the fact that some teleosauroids appear to close the antorbital fenestra completely (e.g., *Machimosaurus*; Young, Hua, et al., 2014). This could be explained if the taxa lacking antorbital fenestrae were interpreted as more terrestrial or inhabited freshwater environments (and potentially losing the salt glands), yet *Machimosaurus hugii* has been interpreted as one of the more pelagic teleosauroids (Krebs, 1968; Young, Hua, et al., 2014). Clarifying this issue will require more detailed investigation of the antorbital region across Thalattosuchia but is beyond the scope of this study.

This work also includes the first description of the olfactory tract and bulbs of a teleosauroid. The olfactory bulbs of *Macrospondylus* appear to be enlarged relative to

those of *Pelagosaurus* or *Cricosaurus*. This may indicate greater reliance on, and greater capacity for, airborne olfaction in teleosauroids than in the more aquatically adapted metriorhynchoids. A greater olfactory capability in teleosauroids would match with their inferred ecology as they would have been considerably more semi-aquatic (and thus spent more time on land) than the more pelagic metriorhynchoids (Johnson et al., 2020b). Additional information from the olfactory region of teleosauroids inferred to have evolved into more pelagic ecologies (e.g., *Bathysuchus megarhinus*, *Aeolodon priscis* [Foffa et al., 2019]) would help test whether olfactory bulb size decreases with increased pelagic capabilities, or whether larger olfactory bulbs of teleosauroids are simply a phylogenetic difference.

5 | CONCLUDING REMARKS

The new information on the cranial and endocranial anatomy of MCZ PVRA-1063 adds to the growing pool of data for phylogenetic, taxonomic, and functional inference in crocodylomorph evolution. The novel endocranial information provided by this specimen advances our understanding of how thalattosuchians adapted to the marine realm following a transition from terrestrial ancestors. Additional sampling across Thalattosuchia will help in assessing the pace and extent of these adaptations through the temporal duration of the clade, and comparisons with other marine crocodylomorph groups (e.g., Dyrosauridae) could test for the presence of common adaptive strategies following marine transitions.

ACKNOWLEDGMENTS

We thank the following people for access to specimens: J. Cundiff and C. Capobianco (MCZ), L. Steel and S. Chapman (NHMUK), R. Allain (MNHN), P. Jeffery, and D. Siveter (OUM), X. Xu and F. Zheng (IVPP), O. Rauhut and M. Moser (SNSB-BSPG), R. Schoch, R. Boettcher, and M. Rasser (SMNS), P. Havlik (GPIT), R. Hauff (UH), D. Schwarz-Wings (MNHB), D. Ehret and *R. Pellegrini* (NJSM). We thank L. Betti-Nash for assistance in editing photographs for use in figures. We thank Y. Herrera and an anonymous reviewer for comments that improved the manuscript and C. Holliday for handling the manuscript. Grant sponsor: National Science Foundation; Grant number: DEB 1754596.

AUTHOR CONTRIBUTIONS

Eric Wilberg: Conceptualization; data curation; funding acquisition; investigation; supervision; visualization; writing - original draft; writing-review & editing. **Alexander Beyl:** Data curation; investigation; visualization; writing - original draft; writing-review & editing. **Stephanie Pierce:** Data curation; resources; writing-review & editing. **Alan Turner:** Conceptualization; data curation; funding acquisition; methodology; project administration; resources; software; visualization; writing - original draft; writing-review & editing.

DATA AVAILABILITY STATEMENT

CT scan and digital model data available by request (https://mczbase.mcz.harvard.edu/guid/MCZ:VP:VPRA-1063). Requests should be directed to mcz_vertebratepaleo@fas.harvard.edu.

ORCID

Eric W. Wilberg https://orcid.org/0000-0002-7038-0825
Alexander R. Beyl https://orcid.org/0000-0002-4428-2076

REFERENCES

Aiglstorfer, M., Havlik, P., & Herrera, Y. (2020). The first metriorhynchoid crocodyliform from the Aalenian (Middle Jurassic) of Germany, with implications for the evolution of Metriorhynchoidea. *Zoological Journal of the Linnean Society*, *188*, 522–551.

Andrews, C. W. (1909). XXXVIII.—On some new Steneosaurs from the Oxford clay of Peterborough. *Annals and Magazine of Natural History*, *3*, 299–308.

Andrews, C. W. (1913). *A descriptive catalogue of the marine reptiles of the Oxford clay, part II*. London: British Museum (Natural History).

Balanoff, A. M., Bever, G. S., Colbert, M. W., Clarke, J. A., Field, D. J., Gignac, P. M., … Witmer, L. M. (2016). Best practices for digitally constructing endocranial casts: Examples from birds and their dinosaurian relatives. *Journal of Anatomy*, *229*, 173–190.

Ballell, A., Moon, B. C., Porro, L. B., Benton, M. J., & Rayfield, E. J. (2019). Convergence and functional evolution of longirostry in crocodylomorphs. *Palaeontology*, *62*, 867–887.

Barrientos-Lara, J. I., Alvarado-Ortega, J., & Fernández, M. S. (2018). The marine crocodile *Maledictosuchus* (Thalattosuchia, Metriorhynchidae) from the Kimmeridgian deposits of Tlaxiaco, Oaxaca, southern Mexico. *Journal of Vertebrate Paleontology*, *38*, 1–14.

Barrientos-Lara, J. I., Herrera, Y., Fernández, M. S., & Alvarado-Ortega, J. (2016). Occurrence of *Torvoneustes* (Crocodylomorpha, Metriorhynchidae) in marine Jurassic deposits of Oaxaca, Mexico. *Revista Brasileira de Paleontologia*, *19*, 415–424.

Bona, P., Degrange, F. J., & Fernández, M. S. (2013). Skull anatomy of the bizarre crocodylian *Mourasuchus nativus* (Alligatoridae, Caimaninae). *The Anatomical Record*, *296*, 227–239.

Brochu, C. A. (2001). Progress and future directions in archosaur phylogenetics. *Journal of Paleontology*, *75*, 1185–1201.

Brusatte, S. L., Muir, A., Young, M. T., Walsh, S., Steel, L., & Witmer, L. M. (2016). The braincase and neurosensory anatomy of an early Jurassic marine crocodylomorph: Implications for crocodylian sinus evolution and sensory transitions. *The Anatomical Record*, *299*, 1511–1530.

Buchy, M.-C., Vignaud, P., Frey, E., Stinnesbeck, W., & Gonzalez Gonzalez, A. H. (2006). A new thalattosuchian crocodyliform from the Tithonian (Upper Jurassic) of northeastern Mexico. *Comptes Rendus Palevol*, *5*(6), 785–794.

Buchy, M.-C., Young, M. T., & Andrade, M. B. (2013). A new specimen of *Cricosaurus saltillensis* (Crocodylomorpha: Metriorhynchidae) from the upper Jurassic of Mexico: Evidence for craniofacial convergence within Metriorhynchidae. *Oryctos*, *10*, 9–21.

Buffetaut, E. (1980). Teleosauridae et Metriorhynchidae l'évolution de deux familles de crocodiliens mésosuchiens marins du Mésozoïque. *Comptes Rendus du 105e Congrés National des Sociétés Savantes*, *3*, 11–22.

Buffetaut, E. (1982). Radiation evolutive, paleoecologie et biogeographie des crocodiliens mesosuchiens. *Memoires de la Societe Geologique de France*, *142*, 1–88.

Busbey, A. B. (1995). The structural consequences of skull flattening in crocodilians. In J. J. Thomason (Ed.), *Functional morphology in vertebrate paleontology* (pp. 173–192). Cambridge, UK: Cambridge University Press.

Cau, A., & Fanti, F. (2011). The oldest known metriorhynchid crocodylian from the middle Jurassic of North-Eastern Italy: Neptunidraco ammoniticus gen. Et sp. nov. *Gondwana Research*, *19*, 550–565.

Chapman, W. (1758). An account of the fossile bones of an alligator, found on the sea-shore, near Whitby in Yorkshire. *Philosophical Transactions of the Royal Society of London*, *50*, 688–691.

Clark, J. M. (1986). Phylogenetic relationships of the crocodylomorph archosaurs. In *Department of Anatomy* (p. 556). University of Chicago, Chicago.

Clark, J. M. (1994). Patterns of evolution in mesozoic crocodyliformes. In N. C. Fraser & H.-D. Sues (Eds.), *In the shadow of the dinosaurs: Early mesozoic tetrapods* (pp. 84–97). New York: Cambridge University Press.

Colbert, E. H. (1946). The eustachian tubes in the Crocodilia. *Copeia*, *1*, 11–14.

Costidis, A., & Rommel, S. A. (2012). Vascularization of air sinuses and fat bodies in the head of the bottlenose dolphin (*Tursiops truncatus*): Morphological implications on physiology. *Frontiers in Physiology*, *3*, 243.

Cuvier, G. (1824). *Recherches sur les ossemens fossiles, où l'on rétablit les caractères de plusieurs animaux dont les révolutions du globe ont détruit les espèces* (2nd ed.). Paris: G. Dufour et E. d'Ocagne.

Dufeau, D. L., & Witmer, L. M. (2015). Ontogeny of the middle-ear air-sinus system in *Alligator mississippiensis* (Archosauria: Crocodylia). *PLoS One*, *10*, e0137060.

Erb, A., & Turner, A. H. (2021). Braincase anatomy of the Paleocene crocodyliform *Rhabdognathus* revealed through high resolution computed tomography. *PeerJ*, *9*, e11253.

Eudes-Deslongchamps, E. (1863-1869). *Notes Paléontologiques*. Caen and Paris: Le Blanc-Hardel et Savy.

Fernández, M., & Gasparini, Z. (2000). Salt glands in a Tithonian metriorhynchid crocodyliform and their physiological significance. *Lethaia*, *33*, 269–276.

Fernández, M., & Gasparini, Z. (2008). Salt glands in the Jurassic Metriorhynchid *Geosaurus*: Implications for the evolution of osmoregulation in Mesozoic marine crocodyliforms. *Naturwissenschaften*, *95*, 79–84.

Fernández, M. S., Carabajal, A. P., Gasparini, Z., & Chong, D. G. (2011). A metriorhynchid crocodyliform braincase from northern Chile. *Journal of Vertebrate Paleontology*, *31*, 369–377.

Fernández, M. S., & Herrera, Y. (2009). Paranasal sinus system of *Geosaurus araucanensis* and the homology of the antorbital fenestra of metriorhynchids (Thalattosuchia: Crocodylomorpha). *Journal of Vertebrate Paleontology*, *29*, 702–714.

Foffa, D., Johnson, M. M., Young, M. T., Steel, L., & Brusatte, S. L. (2019). Revision of the late Jurassic deep-water teleosauroid crocodylomorph *Teleosaurus megarhinus* Hulke, 1871 and evidence of pelagic adaptations in Teleosauroidea. *PeerJ*, *7*, e6646.

Foffa, D., & Young, M. T. (2014). The cranial osteology of *Tyrannoneustes lythrodectikos* (Crocodylomorpha: Metriorhynchidae) from the middle Jurassic of Europe. *PeerJ*, *2*, e608.

Fonseca, P. H. M., Martinelli, A. G., Marinho, T. S., Ribeiro, L. C. B., Schultz, C. L., & Soares, M. B. (2020). Morphology of the endocranial cavities of *Campinasuchus dinizi* (Crocodyliformes: Baurusuchidae) from the upper cretaceous of Brazil. *Geobios*, *58*, 1–16.

Gasparini, Z., Cichowolski, M., & Lazo, D. G. (2005). First record of *Metriorhynchus* (Reptilia: Crocodyliformes) in the Bathonian (middle Jurassic) of the eastern Pacific. *Journal of Paleontology*, *79*, 801–805.

Gasparini, Z., Pol, D., & Spalletti, L. A. (2006). An unusual marine crocodyliform from the Jurassic-Cretaceous boundary of Patagonia. *Science*, *311*, 70–73.

Gasparini, Z., Vignaud, P., & Chong, G. (2000). The Jurassic Thalattosuchia (Crocodyliformes) of Chile: A paleobiogeographic approach. *Bulletin de la Société Géologique de France*, *171*, 657–664.

Geoffroy Saint-Hilaire, E. (1825). Recheres sur l'organisation des gavials, sur leurs affinités naturelles desquelles résulte la nécessité d'une autre distribution générique: *Gavialis*, *Teleosaurus*, *Steneosaurus*: et sur cette question, si les gavials (*Gavialis*), aujourd'hui répandus dans les parties orientales de l'Asie, descendent, par voie non interrompue de génération, des gavials antidiluviens, soit des gavials fossiles, dits crocodiles de Caen (*Teleosaurus*), soit des gavials fossiles du Havre et de Honfleur (*Steneosaurus*). *Mémoires du Muséum National d'Histoire Naturelle*, *12*, 97–155 155–156.

Gerstberger, R. (1991). Partial uncoupling of salt gland blood flow and secretion in the Pekin duck (*Anas platyrhynchos*). *Journal of Physiology*, *435*, 175–186.

Herrera, Y. (2015). Metriorhynchidae (Crocodylomorpha, Thalattosuchia) from upper Jurassic-lower cretaceous of Neuquén Basin (Argentina), with comments on the natural casts of the brain. In M. Fernández & Y. Herrera (Eds.), *Reptiles Extintos: Volumen en Homenaje a Zulma Gasparini* (pp. 159–171). Buenos Aires: Publicación Electrónica de la Asociación Paleontológica Argentina.

Herrera, Y., Fernández, M., & Varela, J. A. (2009). Morfología del miembro anterior de *Geosaurus araucanensis* Gasparini y Dellapé, 1976 (Crocodyliformes: Thalattosuchia). *Ameghiniana*, *46*, 657–667.

Herrera, Y., Fernández, M. S., & Gasparini, Z. (2013a). Postcranial skeleton of *Cricosaurus araucanensis* (Crocodyliformes: Thalattosuchia): Morphology and palaeobiological insights. *Alcheringa: An Australasian Journal of Palaeontology*, *37*, 285–298.

Herrera, Y., Fernández, M. S., & Gasparini, Z. (2013b). The snout of *Cricosaurus araucanensis*: A case study in novel anatomy of the nasal region of metriorhynchids. *Lethaia*, *46*, 331–340.

Herrera, Y., Fernández, M. S., Lamas, S. G., Campos, L., Talevi, M., & Gasparini, Z. (2017). Morphology of the sacral region and reproductive strategies of Metriorhynchidae: A counter-inductive approach. *Earth and Environmental Science Transactions of the Royal Society of Edinburgh*, *106*, 247–255.

Herrera, Y., Gasparini, Z., & Fernández, M. S. (2013). A new Patagonian species of *Cricosaurus* (Crocodyliformes, Thalattosuchia): First evidence of *Cricosaurus* in middle-upper Tithonian lithographic limestone from Gondwana. *Palaeontology*, *56*, 663–678.

Herrera, Y., Gasparini, Z., & Fernández, M. S. (2015). *Purranisaurus potens* Rusconi, an enigmatic metriorhynchid from the late Jurassic-early cretaceous of Neuquén Basin. *Journal of Vertebrate Paleontology*, *35*, e904790.

Herrera, Y., Leardi, J. M., & Fernandez, M. S. (2018). Braincase and endocranial anatomy of two thalattosuchian crocodylomorphs and their relevance in understanding their adaptations to the marine environment. *PeerJ*, *6*, e5686.

Herrera, Y., & Vennari, V. V. (2015). Cranial anatomy and neuroanatomical features of a new specimen of Geosaurini (Crocodylomorpha: Metriorhynchidae) from west-central Argentina. *Historical Biology*, *27*, 33–41.

Holliday, C. M. (2006). *Evolution and function of the jaw musculature and adductor chamber of archosaurs (crocodilans, dinosaurs, and birds)* (p. 325). Department of Biological Sciences, Ohio University, Athens, OH.

Holliday, C. M., & Nesbitt, S. J. (2013). Morphology and diversity of the mandibular symphysis of archosauriforms. *Geological Society, London, Special Publications*, *379*, 555–571.

Holliday, C. M., Porter, W. R., Vliet, K. A., & Witmer, L. M. (2019). The frontoparietal fossa and dorsotemporal fenestra of archosaurs and their significance for interpretations of vascular and muscular anatomy in dinosaurs. *The Anatomical Record*, *303*, 1060–1074.

Holliday, C. M., & Witmer, L. M. (2009). The epipterygoid of crocodyliforms and its significance for the evolution of the orbitotemporal region of eusuchians. *Journal of Vertebrate Paleontology*, *29*, 715–733.

Hua, S. (2020). A new specimen of *Teleidosaurus calvadosii* (Eudes-Deslongchamps, 1866) (Crocodylia, Thalattosuchia) from the middle Jurassic of France. *Annales de Paléontologie*, *106*, 102423.

Hua, S., & Buffetaut, E. (1997). Part V. Crocodylia. In J. M. Callaway & E. L. Nicholls (Eds.), *Ancient Marine Reptiles* (pp. 357–374). San Diego: Academic Press.

Hua, S., & de Buffrenil, V. (1996). Bone histology as a clue in the interpretation of functional adaptations in the Thallatosuchia (Reptilia, Crocodylia). *Journal of Vertebrate Paleontology*, *16*, 703–717.

Hua, S., Vignaud, P., Atrops, F., & Clément, A. (2000). *Enaliosuchus macrospondylus* Koken, 1883 (Crocodylia, Metriorhynchidae) du Valanginien de Barret-le-bas (Hautes Alpes, France): un cas unique de remontée des narines externes parmi les crocodiliens. *Geobios*, *33*, 467–474.

Iordansky, N. N. (1964). The jaw muscles of the crocodiles and some relating structures of the crocodilian skull. *Anatomischer Anzeiger*, *115*, 256–280.

Iordansky, N. N. (1973). The skull of the Crocodylia. In C. Gans & T. Parsons (Eds.), *Biology of the Reptilia* (pp. 201–260). London: Academic Press.

Jäger, C. F. (1828). *Über die fossile Reptilien, welche in Württemberg aufgefunden worden sind*. Stuttgart: J. B. Metzler.

Johnson, M. M., Young, M. T., & Brusatte, S. L. (2019). Redescription of two contemporaneous mesorostrine teleosauroids (Crocodylomorpha, Thalattosuchia) from the Bathonian of England, and insights into the early evolution of Machimosaurini. *Zoological Journal of the Linnean Society*, *189*, 449–482.

Johnson, M. M., Young, M. T., & Brusatte, S. L. (2020a). Emptying the wastebasket: A historical and taxonomic revision of the Jurassic crocodylomorph *Steneosaurus*. *Zoological Journal of the Linnean Society*, *189*, 428–448.

Johnson, M. M., Young, M. T., & Brusatte, S. L. (2020b). The phylogenetics of Teleosauroidea (Crocodylomorpha, Thalattosuchia) and implications for their ecology and evolution. *PeerJ*, *8*, 1–157.

Johnson, M. M., Young, M. T., Steel, L., Foffa, D., Smith, A. S., Hua, S., … Dyke, G. J. (2017). Re-description of '*Steneosaurus*' *obtusidens* Andrews, 1909, an unusual macrophagous teleosaurid crocodylomorph from the middle Jurassic of England. *Zoological Journal of the Linnean Society*, *182*, 385–418.

Johnson, M. M., Young, M. T., Steel, L., & Lepage, Y. (2015). *Steneosaurus edwardsi* (Thalattosuchia, Teleosauridae), the largest known crocodylomorph of the middle Jurassic. *Biological Journal of the Linnean Society*, *115*, 911–918.

Jouve, S. (2009). The skull of *Teleosaurus cadomensis* (Crocodylomorpha; Thalattosuchia), and phylogenetic analysis of Thalattosuchia. *Journal of Vertebrate Paleontology*, *29*, 88–102.

Kley, N. J., Sertich, J. J. W., Turner, A. H., Krause, D. W., O'Connor, P. M., & Georgi, J. A. (2010). Craniofacial morphology of Simosuchus clarki (Crocodyliformes: Notosuchia) from the late cretaceous of Madagascar. *Journal of Vertebrate Paleontology*, *30*, 13–98.

Krebs, B. (1968). Le crocodilien *Machimosaurus*. *Servico Geólogico Portugal (Nova Série)*, *14*, 21–53.

Leardi, J. M., Pol, D., & Clark, J. M. (2017). Detailed anatomy of the braincase of *Macelognathus vagans* marsh, 1884 (Archosauria, Crocodylomorpha) using high resolution tomography and new insights on basal crocodylomorph phylogeny. *PeerJ*, *5*, e2801.

Leardi, J. M., Pol, D., & Clark, J. M. (2020). Braincase anatomy of *Almadasuchus figarii* (Archosauria, Crocodylomorpha) and a review of the cranial pneumaticity in the origins of Crocodylomorpha. *Journal of Anatomy*, *237*, 48–73.

Leardi, J. M., Pol, D., & Fernández, M. S. (2012). The antorbital fenestra of Metriorhynchidae (Crocodyliformes, Thalattosuchia): Testing its homology within a phylogenetic framework. *Journal of Vertebrate Paleontology*, *32*, 490–494.

Martin, J. E., Suteethorn, S., Lauprasert, K., Tong, H., Buffetaut, E., Liard, R., … Claude, J. (2019). A new freshwater teleosaurid from the Jurassic of northeastern Thailand. *Journal of Vertebrate Paleontology*, *38*, e1549059.

Martin, J. E., & Vincent, P. (2013). New remains of *Machimosaurus hugii* von Meyer, 1837 (Crocodilia, Thalattosuchia) from the Kimmeridgian of Germany. *Fossil Record*, *16*, 179–196.

Miall, L. C. (1878). *The skull of the crocodile*. London, UK: Macmillan and Co.

Montefeltro, F. C., Andrade, D. V., & Larsson, H. C. E. (2016). The evolution of the meatal chamber in crocodyliforms. *Journal of Anatomy*, *228*, 838–863.

Mueller-Töwe, I. J. (2006). *Anatomy, phylogeny, and paleoecology of the basal thalattosuchians (mesoeucrocodylia) from the Liassic of Central Europe* (p. 422). Johannes Gutenberg-Universität Mainz, Rhineland Palatinate, Germany.

Nesbitt, S. J. (2011). The early evolution of archosaurs: Relationships and the origin of major clades. *Bulletin of the American Museum of Natural History*, *352*, 1–292.

Ösi, A., Young, M. T., Galácz, A., & Rabi, M. (2018). A new large-bodied thalattosuchian crocodyliform from the lower Jurassic (Toarcian) of Hungary, with further evidence of the mosaic acquisition of marine adaptations in Metriorhynchoidea. *PeerJ*, *6*, e4668.

Parrilla-Bel, J., Young, M. T., Moreno-Azanza, M., & Canudo, J. I. (2013). The first metriorhynchid crocodylomorph from the middle Jurassic of Spain, with implications for evolution of the subclade Rhacheosaurini. *PLoS One*, *8*, e54275.

Pierce, S. E., Angielczyk, K., & Rayfield, E. J. (2009a). Morphospace occupation in thalattosuchian crocodylomorphs: Skull shape variation, species delineation and temporal patterns. *Palaeontology*, *52*, 1057–1097.

Pierce, S. E., Angielczyk, K. D., & Rayfield, E. J. (2009b). Shape and mechanics in thalattosuchian (Crocodylomorpha) skulls: Implications for feeding behaviour and niche partitioning. *Journal of Anatomy*, *215*, 555–576.

Pierce, S. E., & Benton, M. J. (2006). *Pelagosaurus typus* Bronn, 1841 (mesoeucrocodylia: Thalattosuchia) from the upper Lias (Toarcian, lower Jurassic) of Somerset, England. *Journal of Vertebrate Paleontology*, *26*, 621–635.

Pierce, S. E., Williams, M., & Benson, R. B. J. (2017). Virtual reconstruction of the endocranial anatomy of the early Jurassic marine crocodylomorph *Pelagosaurus typus* (Thalattosuchia). *PeerJ*, *5*, e3225.

Pol, D., & Gasparini, Z. (2009). Skull anatomy of *Dakosaurus andiniensis* (Thalattosuchia: Crocodylomorpha) and the phylogenetic position of Thalattosuchia. *Journal of Systematic Palaeontology*, *7*, 163–197.

Pol, D., Rauhut, O. W. M., Leucona, A., Leardi, J. M., Xu, X., & Clark, J. M. (2013). A new fossil from the Jurassic of Patagonia reveals the early basicranial evolution and the origins of Crocodyliformes. *Biological Reviews*, *88*, 862–872.

Porter, W. R., Sedlmayr, J. C., & Witmer, L. M. (2016). Vascular patterns in the heads of crocodilians: Blood vessels and sites of thermal exchange. *Journal of Anatomy*, *229*, 800–824.

Sachs, S., Johnson, M. M., Young, M. T., & Abel, P. (2019). The mystery of *Mystriosaurus* Kaup, 1834: Redescribing the poorly known early Jurassic teleosauroid thalattosuchians *Mystriosaurus laurillardi* Kaup, 1834 and *Steneosaurus brevior* Blake, 1876. *Acta Palaeontologica Polonica*, *64*, 565–579.

Schwab, J. A., Young, M. T., Neenan, J. M., Walsh, S. A., Witmer, L. M., Herrera, Y., ... Brusatte, S. L. (2020). Inner ear sensory system changes as extinct crocodylomorphs transitioned from land to water. *Proceedings of the National Academy of Sciences United States of America*, *117*, 10422–10428.

Schwarz-Wings, D. (2014). The feeding apparatus of dyrosaurids (Crocodyliformes). *Geological Magazine*, *151*, 144–166.

Stenfors, L.-E., Sadé, J., Hellström, S., & Anniko, M. (2001). How can the hooded seal dive to a depth of 1000 m without rupturing its tympanic membrane? A morphological and functional study. *Acta Oto-Laryngologica*, *121*, 689–695.

Vignaud P. 1995. Les Thalattosuchia, crocodiles marins du Mésozoic: systématique phylogénétique, paleoécologie, biochronologie et implications paléogéographiques. In. Poitiers, France: Uinversite de Poitiers. p 271.

Walker, A. D. (1990). A revision of *Sphenosuchus acutus* Haughton, a crocodylomorph reptile from the Elliot formation (late Triassic or early Jurassic) of South Africa. *Philosophical Transactions of the Royal Society of London, Series B: Biological Sciences*, *330*, 1–120.

Walsh, S., Barrett, P. M., Milner, A. R., Manley, G. A., & Witmer, L. M. (2009). Inner ear anatomy is a proxy for deducing auditory capability and behavior in reptiles and birds. *Proceedings of the Royal Society of London, Biological Sciences*, *276*, 1355–1360.

Westphal, F. (1961). Zur Systematik der deutschen und englischen Lias-Krokodilier. *Neues Jahrbuch für Geologie und Palaeontologie Abhandlungen*, *113*, 207–218.

Westphal, F. (1962). Die Krokodilier des deutschen und englischen oberen Lias. *Palaeontographica Abt A*, *116*, 23–118.

Wilberg, E. W. (2015a). A new metriorhynchoid (Crocodylomorpha, Thalattosuchia) from the middle Jurassic of Oregon and the evolutionary timing of marine adaptations in thalattosuchian crocodylomorphs. *Journal of Vertebrate Paleontology*, *35*, e902846.

Wilberg, E. W. (2015b). What's in an outgroup? The impact of outgroup choice on the phylogenetic position of Thalattosuchia (Crocodylomorpha) and the origin of Crocodyliformes. *Systematic Biology*, *64*, 621–637.

Wilberg, E. W., Turner, A. H., & Brochu, C. A. (2019). Evolutionary structure and timing of major habitat shifts in Crocodylomorpha. *Scientific Reports*, *9*, 514.

Witmer, L. M., & Ridgely, R. C. (2008). The paranasal air sinuses of predatory and armored dinosaurs (Archosauria: Theropoda and Ankylosauria) and their contribution to cephalic structure. *The Anatomical Record*, *291*, 1362–1388.

Witmer, L. M., Ridgely, R. C., Dufeau, D. L., & Semones, M. C. (2008). Using CT to peer into the past: 3D visualization of the brain and ear regions of birds, crocodiles and nonavian dinosaurs. In H. Endo & E. Frey (Eds.), *Anatomical imaging: Towards a new morphology* (pp. 67–87). Berlin: Springer.

Wooler. (1758). A description of the fossil skeleton of an animal found in the alum rock near Whitby. *Philosophical Transactions of the Royal Society of London*, *50*, 786–790.

Young, M. T., & Andrade, M. B. (2009). What is *Geosaurus*? Redescription of *Geosaurus giganteus* (Thalattosuchia: Metriorhynchidae) from the upper Jurassic of Bayern, Germany. *Zoological Journal of the Linnean Society*, *157*, 551–585.

Young, M. T., Andrade, M. B., Cornée, J.-J., Steel, L., & Foffa, D. (2014). Re-description of a putative early cretaceous "teleosaurid" from France, with implications for the survival of metriorhynchids and teleosaurids across the Jurassic-cretaceous boundary. *Annales de Paléontologie*, *100*, 165–174.

Young, M. T., Andrade, M. B., Etches, S., & Beatty, B. L. (2013). A new metriorhynchid crocodylomorph from the lower Kimmeridge clay formation (late Jurassic) of England, with

implications for the evolution of dermatocranium ornamentation in Geosaurini. *Zoological Journal of the Linnean Society*, *169*, 820–848.

Young, M. T., Beatty, B., Brusatte, S. L., & Steel, L. (2015). First evidence of denticulated dentition in teleosaurid crocodylomorphs. *Acta Palaeontologica Polonica*, *60*, 661–671.

Young, M. T., Bell, M. A., Andrade, M. B., & Brusatte, S. L. (2011). Body size estimation and evolution in metriorhynchid crocodylomorphs: Implications for species diversification and niche partitioning. *Zoological Journal of the Linnean Society*, *163*, 1199–1216.

Young, M. T., Brusatte, S. L., Andrade, M. B., Desojo, J. B., Beatty, B. L., Steel, L., … Schoch, R. R. (2012). The cranial osteology and feeding ecology of the metriorhynchid crocodylomorph genera *Dakosaurus* and *Plesiosuchus* from the late Jurassic of Europe. *PLoS One*, *7*, e44985.

Young MT, Brusatte SL, Ruta M, Andrade MBd. 2010. The evolution of Metriorhynchoidea (Mesoeucrocodylia, Thalattosuchia): An integrated approach using geometric morphometrics, analysis of disparity, and biomechanics. *Zoological Journal of the Linnean Society 158*:801–859.

Young MT, Hua S, Steel L, Foffa D, Brusatte SL, Thuring S, Mateus O, Ruiz-Omenaca JI, Havlik P, Lepage Y, Andrade MBd. 2014. Revision of the late Jurassic teleosaurid genus *Machimosaurus* (Crocodylomorpha, Thalattosuchia). *Royal Society Open Science 1*:140222.

How to cite this article: Wilberg, E. W., Beyl, A. R., Pierce, S. E., & Turner, A. H. (2021). Cranial and endocranial anatomy of a three-dimensionally preserved teleosauroid thalattosuchian skull. *The Anatomical Record*, 1–34. https://doi.org/10.1002/ar.24704